BSMS#1485550, VOL 0, ISS 0

A review on high stiffness aluminum-based composites and bimetallics

Sajjad Amirkhanlou, and Shouxun Ji

QUERY SHEET

This page lists questions we have about your paper. The numbers displayed at left can be found in the text of the paper for reference. In addition, please review your paper as a whole for correctness.

Q1. A disclosure statement reporting no conflict of interest has been inserted. Please correct if this is inaccurate.
Q2. Please provide volume number and page range for the reference "4".
Q3. Please provide publisher location for the references "15, 16, 65, 84, 85".
Q4. Please expand all author names for all references instead of using "et al.".
Q5. Please provide publisher details for the reference "64".

TABLE OF CONTENTS LISTING

The table of contents for the journal will list your paper exactly as it appears below:

CRITICAL REVIEWS IN SOLID STATE AND MATERIALS SCIENCES
https://doi.org/10.1080/10408436.2018.1485550

Taylor & Francis
Taylor & Francis Group

Check for updates

A review on high stiffness aluminum-based composites and bimetallics

Sajjad Amirkhanlou and Shouxun Ji

Brunel Centre for Advanced Solidification Technology (BCAST), Institute of Materials and Manufacturing, Brunel University London, Uxbridge, United Kingdom

ABSTRACT

The Young's modulus of aluminum-based materials is one of the most important mechanical properties in controlling structural performance. The improvement of the Young's modulus of castable aluminum-based materials is essential for improving their competiveness in light weighting structural applications. Currently, there are limited options for cast aluminum alloys with outstanding Young's modulus. Also, for further stiffness improvement and thereby weight lightening, in-depth understanding of the relevant mechanisms for modulus improvement in aluminum alloys is necessary. This review focuses on the Young's modulus of cast aluminum-based composites, as well as aluminum alloys reinforced with continuous metallic fibers (bimetallic materials). The effect of different chemical elements in cast alloys, the constituents of *in-situ* and *ex-situ* formed aluminum matrix composites, and the wire-enhanced bimetallic materials on the Young's modulus of aluminum-based materials are reviewed. The Young's modulus of cast aluminum alloys can be improved by: (a) introducing high modulus reinforcement phases – such as TiB_2, SiC, B_4C, and Al_2O_3 – into aluminum by *in-situ* reactions or by *ex-situ* additions; and (b) forming bimetallic materials with metallic wire/bar reinforcement in the aluminum matrix. The performance of a stiff aluminum alloy depends on the volume fraction, size, and distribution of the high modulus phases as well as the interface between reinforcement and Al matrix. One of the major concerns is the reduction of the ductility of castings after adding specific high modulus phases to increase the Young's modulus. Further research into the improvement of Young's modulus and the ductility of aluminum alloys is necessary through proper selection of reinforcement, optimizing interface, and distribution of reinforcement.

KEYWORDS

Cast aluminum alloys; stiffness; high modulus materials; bimetallic materials; metal matrix composites; light metals

Table of contents

CONTACT Shouxun Ji Shouxun.Ji@brunel.ac.uk
Color versions of one or more of the figures in the article can be found online at www.tandfonline.com/bsms.
© 2018 Taylor &Francis Group, LLC

1. Introduction

Weight reduction through applying aluminum structural components in aerospace and automobile industries is one of the most promising ways to decrease energy and fuel consumption.[1,2] These structural components, in particular shaped castings, are usually designed on the criteria of either yield strength or stiffness.[3,4] When the yield strength is used as the design criterion, aluminum alloys with much higher strength than pure aluminum are commercially available and these can be selected for industrial applications.[5,6] However, when the stiffness is used as the design criterion, there are limited options for the aluminum alloys with significantly increased stiffness than that of aluminum.[7,8] There is a lack of thorough understanding of the stiffness of aluminum alloys and aluminum-based materials that can be used to make castings. Moreover, some of the strengthening mechanisms, which result in a significant improvement in yield strength, have no obvious effect on the stiffness.[9,10] This has limited the applications of aluminum alloys in the shaped castings and components that require high modulus to achieve further weight reduction in the aluminum structures.

As the intrinsic property of materials, the Young's modulus of cast aluminum alloys can only be marginally influenced by manipulating traditional metallurgical variables that can change the microstructure of aluminum alloys significantly.[11,12] Minor changes of microstructure by alloying elements as well as deformation and heat treatment processes cannot improve the stiffness of Al-based materials. Lucena et al.[13] studied the variation in the Young's modulus of AA1050 (>99.5% Al) with cold plastic deformation (tension test). Young's modulus decreased from 69 GPa (initial material) to 63 GPa (2.5% strain), then increased to 65% (6% strain) and finally stabilized to 66 GPa (13% strain). Villuendas et al.[14] showed that the Young's modulus of AA2024 and AA7075 in solution treated, deformed, and aged alloys were slightly lower (<2% reduction) than those of the undeformed specimens. Despite of deformation and heat treatment, chemical composition and phase constituents are two main factors governing the stiffness properties of casting alloys.[15] Processes that can change the microstructure significantly can alter the Young's modulus. The high concentration of alloying elements can have perceptible influence through the contribution in bind interaction. In fact, the high modulus phases can be introduced into the aluminum matrix through major addition of alloying elements and/or ceramic particles.[16,17] The addition of ceramics into the aluminum matrix to form aluminum matrix composites (AMCs) has been the topic of numerous investigations,[18,19] in which the high modulus phases can be generated by *in-situ* reactions with different metallic elements or nonmetallic ceramic compounds, or by direct injection of foreign phases.[20,21] In a similar way, bimetallic materials such as wire-reinforced metallic structures can be recognized as a special category of composites in macroscale,[22] which can be used for an effective increase of Young's modulus. In general, the Young's modulus of cast aluminum alloys is less sensitive to alloying as compared to the stiffer reinforcement in AMCs or bimetallic materials.

The understanding of the successes and challenges in the stiffness of materials can serve as a guidepost for where future work is needed in order to effectively propel the technology development. Therefore, this review focuses on the Young's modulus of cast aluminum alloys, composites, and bimetallic materials and their fabrication processes, aiming to provide a snapshot of the current progress on cast aluminum alloys for improving their Young's modulus. The paper is outlined as follows. Section two summarizes the effect of wire reinforcement on the Young's modulus of aluminum-based bimetallic materials. The properties of commonly used reinforcements are discussed in association with the merits and limitations of processing. Section three focuses on the stiffness improvement by *in-situ* and *ex-situ* composites. A discussion on the processing, microstructure, and Young's modulus of the *in-situ* and *ex-situ* reinforcement – including TiB_2, TiC, AlN, ZrB_2, and Al_2O_3 – in cast Al alloys is provided. Section five ends the paper with the summary and future outlook.

2. Stiffness improvement in bimetallic materials

Bimetallic materials can be considered as a special type of composites, in which continuous metallic wires/bars are used as skeletons or frames for overcasting with conventional casting methods.[23,24] Overcasting is casting process when liquid molten metal is poured onto a solid-state metal/ceramic.[25] The network structures, or skeletons or continuous fibers, have been extensively used in polymer/ceramic matrix composites,[26,27] but the bimetallic materials are particularly used in this review for the metal–metal mixture made by casting, in which the metallic skeletons or frames made by high modulus reinforcement are covered partially or completely by aluminum alloys. The skeleton preforms not only provide a

PROOF ONLY

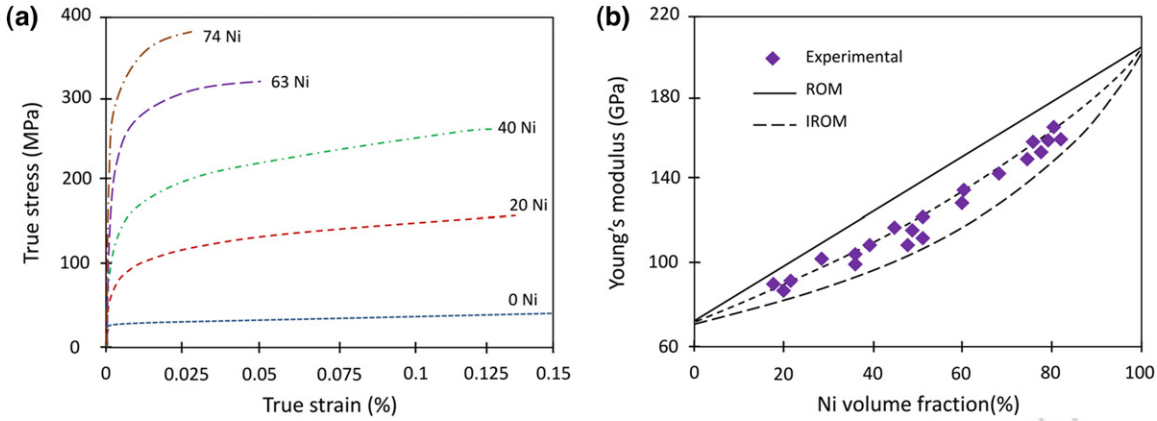

Figure 1. (a) Tensile curves and (b) Young's modulus of pure Al and Al/Ni bimetallic materials.[34]

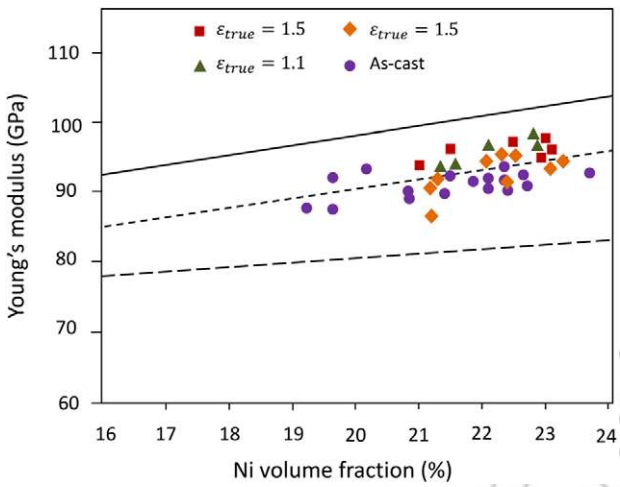

Figure 2. Young's modulus of as-cast and deformed Al/Ni bimetallic materials.[37]

controlled and stable reinforcement, but also offer new architectures and increase the Young's modulus and provide more effective load transfer.[28]

Compared with the reinforcements such as particles,[29] whiskers,[30] short fibers, and continuous fibers[31] used in AMCs, the metallic network structures or skeletons are likely desirable to perform more efficiently, especially in reinforcing the local area of a cast component with relatively low cost and more flexible in manufacturing through casting processes. AMCs usually present low fracture toughness due to the brittle nature of reinforcement, which restricts their applications. The network structure fabricated by metallic wires can be 1D, 2D, or 3D interconnected structures with appropriate surface treatment, which enhance the interface bonding during casting process and improve the modulus without scarifying ductility and toughness. The network structure and the interface are two critical aspects for the manufacturing of sound bimetallic materials. According to the nature of metals, nickel and steel/iron are two popular options for making network structure in the existing literature. Limited studies for other potential metals have been performed.

2.1. Al/Nickel Bimetallic Materials

The interconnected network made by continuous wires of Inconel 601 (12 μm diameter) has been used to reinforce aluminum alloys through sintering the wires before infiltrating aluminum melt by squeeze casting.[32,33] Figure 1(a) shows the stress–strain curves for pure Al and Al/Ni bimetallic materials.[35] The remarkable improvement of ductility is attributed to the absence of defects in the microstructure of the Al/Ni bimetallic materials. Figure 1(b) shows the variation of the Young's modulus of Al/Ni bimetallic materials as a function of the volume fraction of the reinforced wires, in which the upper and lower curves correspond to the ROM and IROM models computed using $E_{Al} = 70$ GPa and $E_{In601} = 206$ GPa. The Young's modulus increases in the bimetallic materials with increasing the Ni volume fraction. Most of the results are close to the average between the two bounds defined by the ROM and IROM models. The Young's modulus can reach a level of 95 GPa, while the elongation is still more than 7% in the Al/30 vol.% Ni wire-reinforced bimetallic materials.[36] The deformation has no significant effect on the Young's modulus of the Al/Ni bimetallic materials, as shown in Figure 2. The Young's modulus under as-cast condition is very similar to that under as-deformed condition,[34] which is due to the fact that heat treatment and metal forming do not change the volume fraction of high modulus phases in the aluminum alloys and thereby negligible change has been reported after these processes.[14]

The interface between Al matrix and wire reinforcement plays a critical role in stiffness

PROOF ONLY

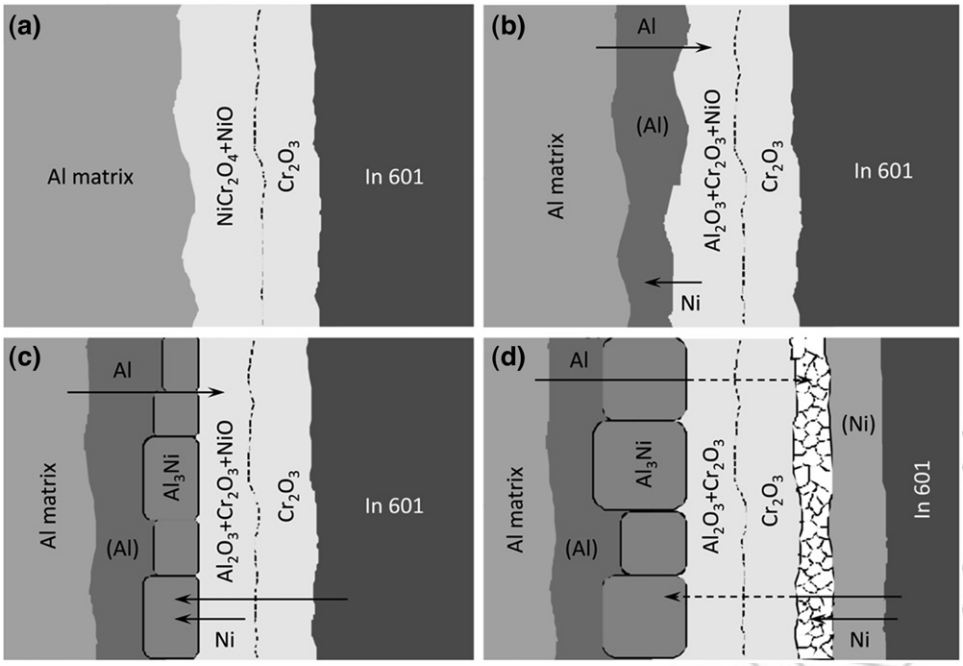

Figure 3. Mechanism of nucleation and growth of the intermetallic nodules in the Al/Ni bimetallic materials.[40]

enhancement in the bimetallic materials. Salmon et al.[38] investigated the influence of the oxidation of Ni wire on the mechanical properties of Al/Ni bimetallic materials and found that an optimum stress and ductility can be obtained with an appropriate oxidation of the Ni alloy during sintering. The mechanical properties can be justified as a result of compromise between the sufficient oxide roughness to the desired wire/matrix adhesion and the limited oxidation to prevent an excessive degradation of the wires. The tensile properties of Al/Ni bimetallic materials are sensitively affected by the nature of the layer of oxide barrier which protects the wires from the reaction with the matrix during casting.[39] The ductility of Al/Ni bimetallic materials can be improved by tuning the annealing conditions during the sintering process and introducing a barrier layer into the Al/Ni interface. It has been found that the partial conversion of the barrier layer into a mixture of $Al_2O_3 + Cr_2O_3$ oxides forms the precipitation of a layer of $NiAl_3$ grains on top of the oxide layer, as shown in Figure 3.[41] When the reduction process of Ni and Fe oxides by Al is completed, Al can diffuse across the oxide layer to form aluminide nodules by reacting with the constituents of the Ni wire. The formation of these nodules can increase the flow strength and the ductility in Al/Ni bimetallic materials.[40,41]

The matrix materials also affect the Young's modulus of the bimetallic materials. Boland et al.[41] investigated the stiffness of cast Al-13 wt.% Si alloy reinforced by Inconel 601 wires. As shown in Figure 4, the

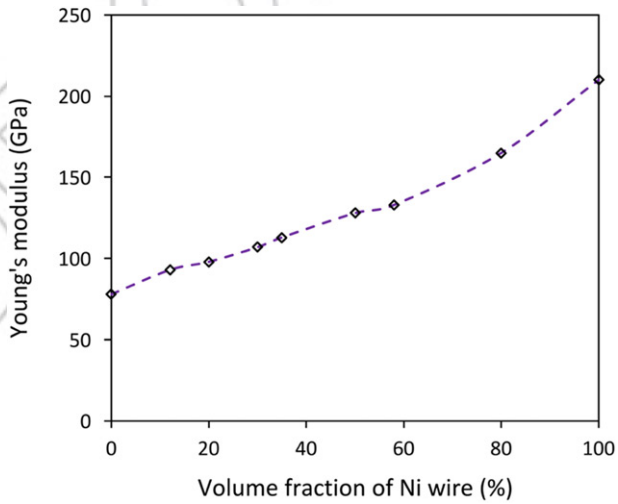

Figure 4. Young's modulus of Al-13 wt.% Si alloy reinforced with Ni wires.[41]

Young's modulus can be significantly increased with the increment of Ni contents in the Al-13 wt.% Si alloy. Comparing the results shown in Figures 1–4, the reinforcement is more effective in the alloys than that in the pure aluminum.

Two parameters are important in the processing of bimetallic materials. One is the initiation of a reaction between the wires and the matrix, which is normally controlled by the cooling rate during casting, and the second is the stability of the oxide passivation barrier at the surface of the wires. The stability of the oxide barrier can be increased either by a pre-oxidizing treatment for the reinforcement wires or by specified

PROOF ONLY

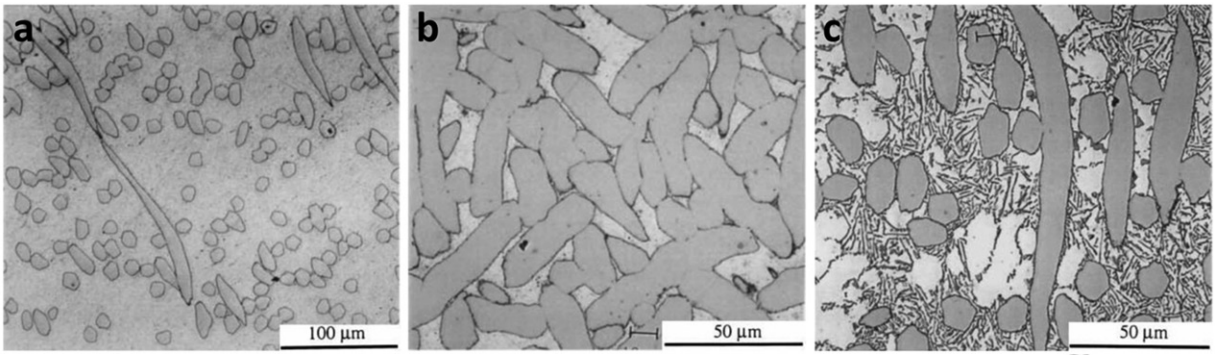

Figure 5. Optical micrograph of (a) Al/20 vol.% Ni, (b) Al/80 vol.% Ni, and (c) Al-13Si/20 vol.% Ni bimetallic materials.[41]

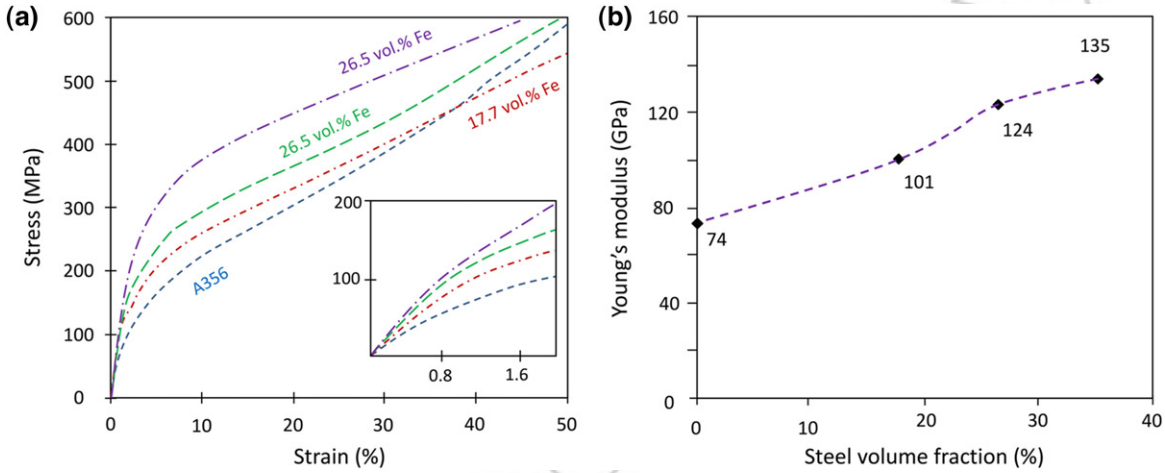

Figure 6. (a) Stress–strain curves for the bimetallic materials with different volume fraction of steel wires and (b) the corresponding Young's modulus.[40]

alloying elements to decrease the melting temperature of the matrix. The Cr-rich passivation layer on the surface of IN601 can increase the refractoriness in oxidizing environments. This will reduce the reactivity of the wires toward Al during overcasting. On the other hand, when the matrix is Al-Si alloys, the Si platelets tend to nucleate preferentially at the wire/matrix interface. This phenomenon has been reported to occur commonly in the composites with SiC, Al_2O_3, or TiB_2 reinforcements with the particle pushing mechanism.[40] Therefore, the presence of Si in Al induces a strong reduction of the reactivity between the wires and the matrix, which can result in the further improvement in the Young's modulus of the bimetallic materials. As illustrated in Figure 5, no reaction compound in the matrix could be detected in the bimetallic materials processed using optimized pre-oxidized preforms.[15] It is necessary to note that the interface requirement is different between the AMCs and the bimetallic materials. In AMCs, the interface is preferred to be clean without any reaction. However, a limited reaction layer is preferred in the bimetallic materials for the better mechanical properties.

2.2. Al/Stainless steel Bimetallic Materials

Fabrication of aluminum-based bimetallic materials reinforced by 3D entangled stainless steel wires has been successful using mono-filament annealed 304 stainless steel wires with 100 µm in diameter in a preform structure.[34,36] The continuous wire was firstly coiled around a ø1.5 mm rod to form spring-like segments, which were subsequently stretched and entangled to form a pre-compacted sample for squeeze casting. The nominal compressive stress–-strain curves are shown in Figure 6. The yield strength and the Young's modulus of the bimetallic material increase as the volume fraction of the steel wires increases. The yield strength can reach 318 MPa for the bimetallic material reinforced with the 35.4 vol.% of entangled stainless steel preform. The Young's modulus of Al/26 vol.% stainless steel bimetallic material is 124 GPa, which shows a significant improvement in comparison with that of the A356 alloy.

The microstructures of A356 matrix alloy reinforced by 3D entangled wires are shown in Figure 7.

PROOF

The wire segments show different morphologies in the matrix with homogeneous distribution. When the process is properly controlled, the introduction of wires has little influence on the microstructures of the matrix. In optimum conditions, the cohesion between the matrix and the wires is well obtained and no obvious traces of interface reaction can be observed because of the prevention of the reaction by the oxide barrier layer on the metallic wire,[42] which offers the best improvement of the Young's modulus.

The network structure of stainless steel can also be fabricated by sintering the wires before infiltrating the aluminum alloys through casting. The improvement of the Young's modulus without significantly scarifying the ductility is achievable in bimetallic materials reinforced by an interconnected network of continuous wires of stainless steel.[41] Figure 8 shows the Young's modulus and the density of Al/steel cast bimetallic materials versus the volume fraction of the interconnected network of continuous wires. It is obvious that the Young's modulus increases with increasing steel volume fraction. When the interconnected structures are used to improve the Young's modulus, the selection of the desirable volume fraction of the reinforcement and the structural design should be considered as important criteria.

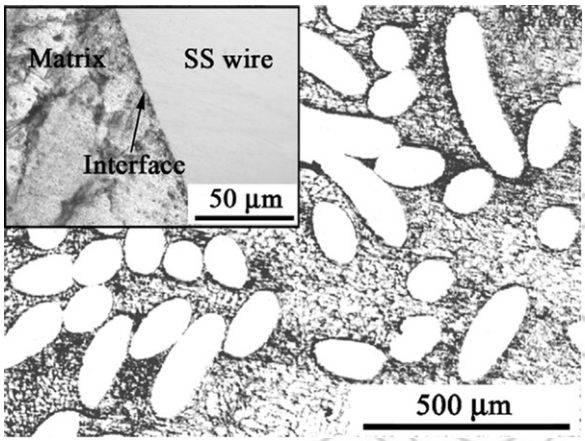

Figure 7. Microstructures of the A356 alloys reinforced by a preform with entangled 304 stainless steel wire at 17.7 vol.%.[40]

2.3. Al/Iron Bimetallic Materials

Interconnected wires in the form of three-dimensional preforms are an approach to improve the Young's modulus by continuous steel/iron reinforcement in Al alloys. Gupta et al.[37,40] fabricated several types of 3D preforms using the galvanized AISI 1008 wire of 0.8 mm diameter coated by 10.8 vol.% zinc. The geometries of the two types of reinforcement preforms are shown in Figure 9.

The mechanical properties for the Al/Fe bimetallic materials with AA1050 (99.5 wt.% Al) as the matrix are shown in Table 1. The incorporation of 3–5 vol.% of iron wires as reinforcement increases the Young's modulus, yield strength, and ultimate tensile strength, but degrades the ductility. The Young's modulus is 88 GPa and the specific stiffness is 30.3 GPa/(g/cm^3) for the Al/5 vol.% Fe bimetallic materials, which is much higher than that of the monolithic Al alloys. The measured Young's modulus of the bimetallic Al/Fe materials exceeds the ROM prediction. This has been attributed to the combined effect of redistributing the fiber stress from the three-dimensional interconnected nature and the limited presence of the intermetallics at the interface.[45] Gupta et al.[40] fabricated aluminum-based bimetallic materials containing titanium particles and iron mesh (continuous) reinforcement. Ti particles and the galvanized iron wire mesh (0.4 vol.% zinc and 0.8 mm wire diameter) are utilized as the continuous/interconnected

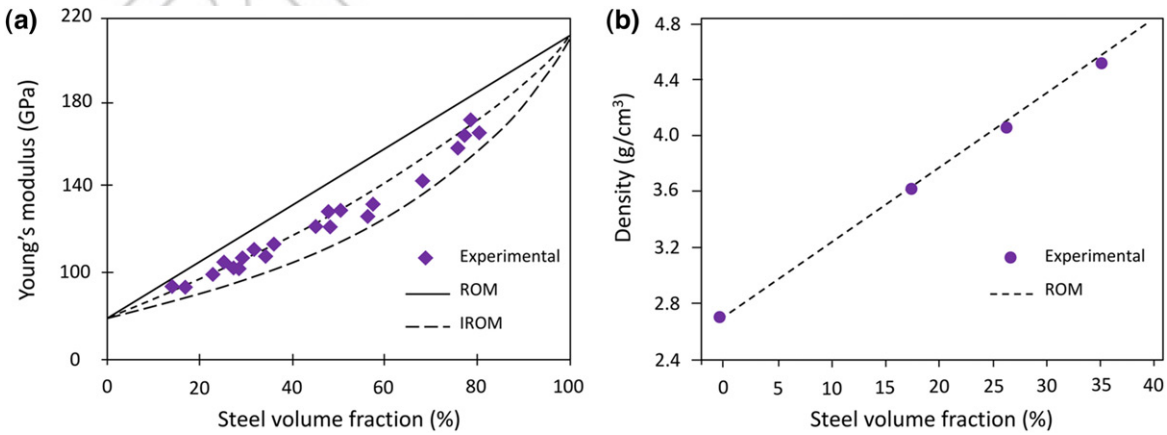

Figure 8. (a) Young's modulus and (b) density of Al-Si/steel cast bimetallic materials with an interconnected network of continuous wires of stainless steel.[36,41]

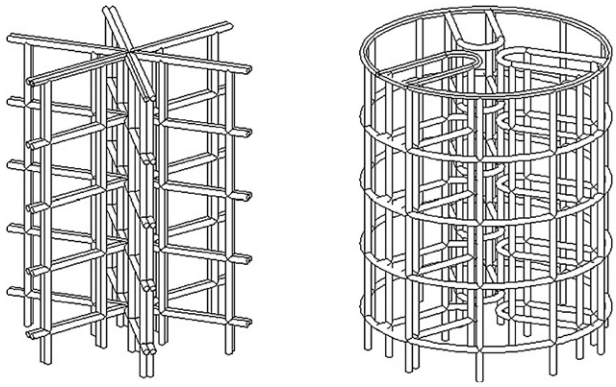

Figure 9. Schematic diagram of two different reinforcement preforms employed in Al/galvanized iron bimetallic materials.[43]

Table 1. Mechanical properties of aluminum reinforced with galvanized iron.[44]

Materials	Young's modulus (GPa)	Yield strength (MPa)	Ultimate tensile strength (MPa)	Ductility (%)	Density (g/cm^3)	Specific stiffness GPa/(g/cm^3)
Al (matrix)	70±2	101±6	120±3	17±9	2.7	25.9
Al/3vol.%Fe*	76±2	108±2	131±4	5±3	2.92	26.1
Al/3vol.%Fe*	81±2	152±4	186±15	5±4	2.81	28.8
Al/3vol.%Fe*	81±2	150±6	173±16	3±2	2.80	28.9
Al/5vol.%Fe	88±1	105±5	130±6	7±3	2.91	30.3

*With different wire arrangement.

reinforcement phase. The presence of reinforcement results in the 7.6% reduction in the coefficient of thermal expansion, the 10% increase in the Young's modulus, the 20% increase in the 0.2% yield strength, and the 27% increase in the ultimate tensile strength.

As the critical characteristics in manufacturing the bimetallic materials, the interface between steel/iron and aluminum has been extensively studied through different approaches due to the avoidance of formation of detrimental phases.[46] The interfaces between steel/iron and aluminum melt can be obtained by immersing the steel/iron into aluminum melt or overcasting aluminum melt onto the steel/iron surface. Dezellus et al.[47] studied the formation of the interface layer, by immersing mild steel into Al-Si alloy melts, and the mechanical properties of interface, by the pushout test. The results showed that the Al_5Fe_2Si and $Al_9Fe_2Si_2$ phases are formed at the interface and the crack initiation would occur in the intermetallic reaction layer. The formation of the intermetallic layer increases the mechanical properties of the bimetallic materials.

Viala et al.[43] and Manasijevic et al.[45] prepared iron base insert reinforced Al-Si alloys by gravity casting and revealed that a continuous metallurgical bond at the iron insert/Al-Si alloy interface can be achieved via the formation of $FeAl_3$ and Fe_2Al_5 intermetallic phases on the interface. Bouayad et al.[48] found that several intermetallic compounds, including γ-Al_3FeSi, η-$Al_5Fe_2(Si)$, and β-Al_5FeSi, can be formed at the interface. The types of reaction products depend on the times and temperatures. Kobayashi and Yakou[49] reported that the common sequence to form the reaction layer is $Fe/Fe_2Al_5/FeAl_3/Al$, but Zhang et al.[50] showed that the sequence of the reaction layer is Fe/η-$Al_5Fe_2(Si)$/β-Al_5FeSi/Al–Si. The experimental results have confirmed that the surface modification of aluminizing can promote the formation of sound surface and metallurgical bonding between steel and Al, which can be achieved by compound casting. Arghavani et al.[51] found that the Zn coating on the steel surface could enhance the wettability of bonding surface between steel and A5052 Al alloy. Liu et al.[52,53] found that the intermetallic compounds $Al_5Fe_2Zn_x$ and Al_3FeZn_x are formed at the interface between hot-dip galvanized steel and pure Al after compound casting. Generally, the zincate must be at an appropriate thickness for the reaction during overcasting. If the thickness is more than the diffusion distance, the Zn layer will still exist in the final microstructure after casting, which is detrimental to the mechanical properties. This has been partially confirmed by Schwankl et al.[54] showing that the interface strength determined by zinc is the weakest part of the compound castings. If the coating is too thin, there are no sufficient compounds to provide bonding strength. Therefore, the bonding interface between the iron/steel and the aluminum alloy is the determining factor for manufacturing the bimetallic materials.

2.4. Other Bimetallic Materials

The Young's modulus of Al-based bimetallic materials reinforced by other metals can be roughly estimated by the ROM model and the results are shown in Figure 10. Comparing with the Young's modulus of Fe and Ni at a level of ~200 GPa, the other continuous reinforcement – such as W and Mo – has a higher potential for the improvement of stiffness. However, the cost and processing procedure will remain an issue in its application.

3. Stiffness improvement in aluminum-based composites

Aluminum matrix composites reinforced with particles, short fibers/whiskers, or continuous fibers have received considerable attention over the past decades due to the attractive properties resulting from the

PROOF ONLY

combination of their constituents.[55–57] Al/TiB_2, Al/TiC, Al/ZrB_2, Al/SiC, Al/AlN, Al/Al_2O_3, and Al/Mg_2Si have been reported to be able to improve the Young's modulus of cast Al alloys.[58–60] The improvement of Young's modulus in AMCs can be successfully achieved through a variety of casting processes, including gravity casting, stirring casting, investment casting, die casting, vacuum-assisted casting, semi-solid casting, and squeeze casting for manufacturing shaped components, or making billets by direct chill casting for further processing such as forging, extrusion or rolling.

The Young's modulus of pure aluminum can be enhanced from 70 to 240 GPa by the reinforcement of 60 vol.% continuous fiber.[19] Similarly, the castings of Al-9Si/20 vol.% SiC_p composites significantly improve the Young's modulus with the wear resistance equivalent or better than that of gray cast irons.[61] Discontinuously reinforced AMCs have been demonstrated to offer essentially isotropic properties with substantial improvements in stiffness and strength. However, a 50% increase in the Young's modulus of Al alloys can be achieved by substituting a discontinuous reinforcement with continuous ones in AMCs.[62] It is therefore capable of incorporating appropriate reinforcement in suitable volume fractions for casting aluminum components with improved Young's modulus and other technological properties such as high thermal conductivity, high specific strength, tailorable coefficient of thermal expansion, improved strength, and low density, which is dependent upon the composition, grain size, microstructure, and fabrication process.

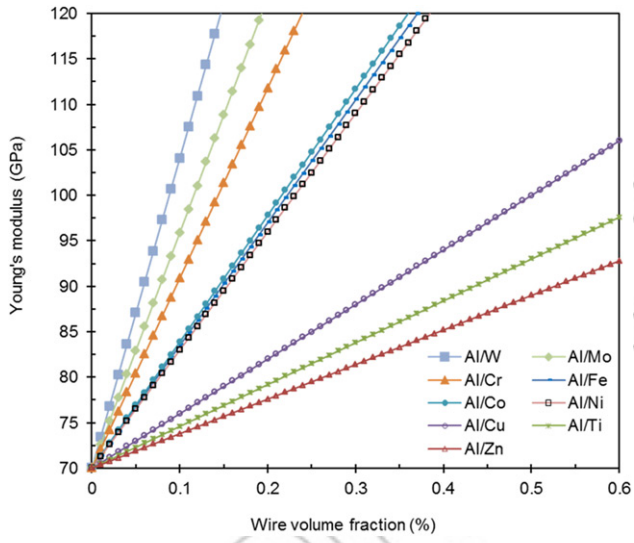

Figure 10. Young's modulus of aluminum-based bimetallic materials reinforced with different types of metallic wires estimated by rule of mixtures.

The stiffness property of some reinforcement phases is listed in Table 2. These phases show the much-increased Young's modulus and melting point in comparison with pure aluminum. In AMCs, the reinforcement phase can be formed by *in-situ* reaction or by *ex-situ* additions. In the specific condition, the *in-situ* particles can act as nucleating sites for grain refinement or as strengthening phases to hinder dislocation motion.[65,66] Currently, several fabrication methods including liquid state processing, deposition process, and solid-state processing have been developed for the manufacture of AMCs. Figure 11 shows the detailed casting process routes for manufacturing AMCs, which include infiltration techniques,[67,68] stirring techniques,[69,70] and rapid solidification.[71,72] Liquid state processing is usually involved with the casting process, which is energy-efficient and cost-effective for massive production. Products of complex shape can be formed directly through the melt mixture with reinforcement. It is very attractive to produce as-cast components of AMCs with a uniform reinforcement distribution of individual particles and structural integrity. However, during solidification, the particles ahead of the interface may get pushed, engulfed, or entrapped in the moving solidification front. The other difficulties in the casting process are the non-wettability of *ex-situ* particles by liquid metal,

Table 2. Properties of typical reinforcements.[63–64]

Reinforcement	Melting point (°C)	Young's modulus (GPa)	UTS (MPa)	Density (g/cm^3)	Thermal conductivity (W/m·K)	Coff. of thermal expansion (10^{-6}/K)
ZrB_2	3246	350		6.09	140	7.4
AlN	2200	330	2,100	3.26	150	3.3
Al_2O_3	2043	380	2,070	3.15	30	7.0
TiC	3067	400	1,540	4.90	110	9.0
TiB_2	3225	560	3,300	4.52	24	8.0
Mg_2Si	1102	120		4.50	4.4	7.5
ZrO_2	2715	350	2,070	4.84	3.3	7.0
B_4C	2763	425	2,690	2.35	39	3.5
SiC	2730	450	2,280	3.21	120	3.4
VC	2810	430		5.77		4.1
WC	2870	640	500	15.52	60	5.1
Si_3N_4	1900	207	530	3.18	28	1.5

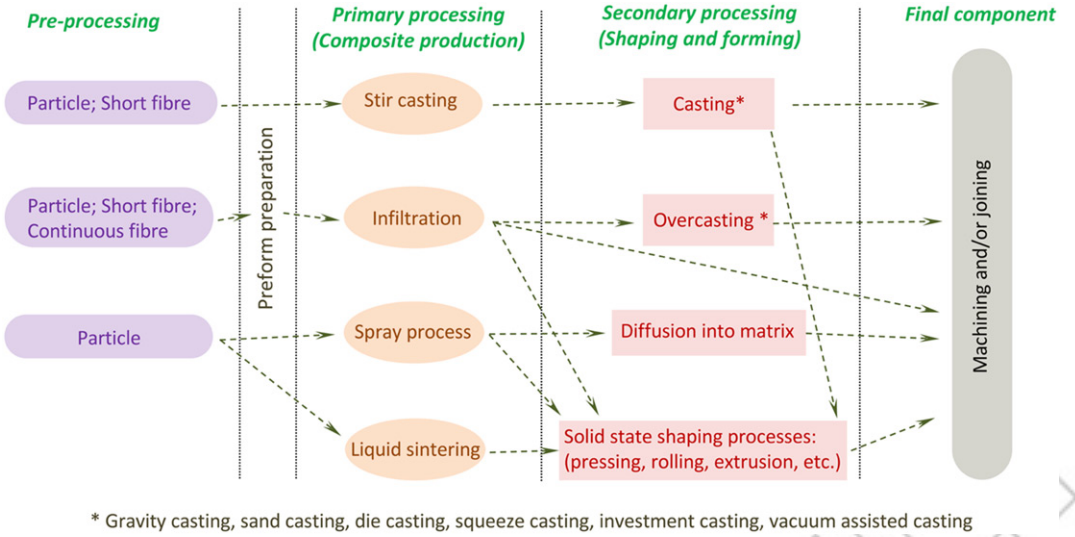

Figure 11. Schematic diagram of processing methods of AMCs.

and the particle–Al interface interaction. Although the addition of Ni, Mg, Li, Si, and Ca into Al melt can improve wettability either by changing the interfacial energy through some interfacial reaction or by modifying the oxide layer on the metal surface,[73–75] the difficulty to obtain uniform dispersion of reinforcement particles is still an issue that hinders the adoption of AMCs in industry.[76,77]

In order to effectively improve the Young's modulus of AMCs, the generation of high modulus phases, the reinforcement phases with covalent and ionic interatomic bonds in aluminum alloys are preferred approaches according to the nature of stiffness.[78,79] Therefore, the *in-situ* method is better than the *ex-situ* method because the wettability between the *in-situ* formed phases and the aluminum matrix is significantly higher and is capable of forming clean and strong interfacial bonding in between.[80,81] However, the *in-situ* method is suitable for particulate-reinforced AMCs because the *in-situ* techniques are not capable of making continuous fiber-reinforced AMCs.

The Young's modulus of composite materials can be estimated by theoretical modeling, which depends on the morphological arrangement of materials components. The most frequently used mathematical models include: (a) the rule of mixtures (ROM) and the inverse rule of mixtures (IROM),[82] (b) the Halpin–Tsai model,[83] (c) the Hashin–Shtrikman model,[84] and (d) the Tuchinskii model.[85] The ROM (upper bound) and IROM (lower bound) can be obtained according to the equal strain assumption and the equal stress assumption, respectively.[16] The elastic properties of all of the composites are usually located between the ROM upper and IROM lower bounds.[86] The Halpin–Tsai model has a more complicated mathematical structure than that of the ROM or IROM. In this model, the modulus of elasticity and the volume fraction of the components and the aspect ratio (ratio of the geometric dimensions) of the reinforcement are taken into account. It has been widely reported that Halpin–Tsai model is more accurate for particulate metal matrix composites. In the Hashin and Shtrikman (H-S) theorem,[86] the upper bound rigorously corresponds to the composites containing the 'soft' inclusion matrix phase encapsulated by a 'stiffer' reinforcement phase, while the lower bound corresponds to the composites with a 'stiffer' inclusion reinforcement phase encapsulated by a 'softer' matrix phase. The H-S bounds are tighter than the ROM bounds and have been regarded as the best possible bounds on properties for isotropic two-phase composites. The Tuchinskii model[87] considers a two-phase interpenetrating skeletal structure. The calculated value of modulus can be a good estimation of experimental guidance. However, this review will not focus the modeling approaches and principles. Some existing results from modeling are used to review the experimental data.

3.1. Al/TiB_2 Composites

TiB_2 is one of the most popular reinforcements for high modulus AMCs because of its Young's modulus of 560 GPa and its easy synthesis using an *in-situ* process.[87] The *in-situ* formed TiB_2 offers a better interface with the aluminum matrix than the *ex-situ* added particles.[88,89] The *in-situ* Al/TiB_2 composites can be synthesized using K_2TiF_6 and KBF_4 salt reactions in molten Al;[90] through a self-propagating high-temperature synthesis (SHS) reaction via Al-Ti-B powder

PROOF ONLY

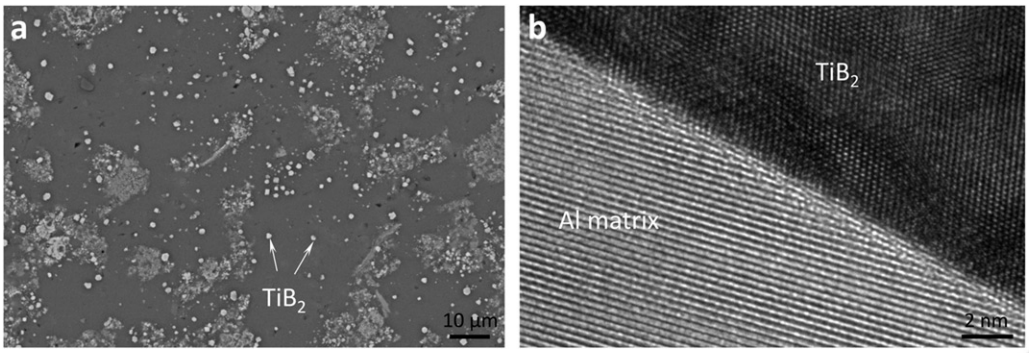

Figure 12. (a) A SEM micrograph of the Al-9Si-1Mg-0.7Cu/TiB_2 composite with 14 wt.% TiB_2 particles and (b) a TEM micrograph showing the clean and well-bonded interface between the α-Al and TiB_2 particles.[102]

compact/preform added to molten Al;[91–93] through the reaction of TiO_2-H_3BO_3-Na_3AlF_6 with Al;[94] or via chemical reactions among Al, TiO_2, and B_2O_3 particles.[95] It is generally believed that the presence of a Al_3Ti phase in Al/TiB_2 composites is beneficial for grain refinement but is detrimental to the mechanical properties.[96] The Al_3Ti can be eliminated during synthesis by the proper control of temperature, time, and ratios of the raw materials.[91,97] The presence of Si in cast Al alloys can improve the dispersion of TiB_2 particles,[98] although the TiB_2 particles are still partially segregated in the eutectic regions because of the pushing mechanism during solidification.[99–101] The typical microstructure of Al/TiB_2 composites is shown in Figure 12. The Al-9Si-1Mg-0.7Cu/TiB_2 composite can be produced with clean, smooth, and well-bonded interfaces between the aluminum matrix and TiB_2 particles between 25 and 3,000 nm.[103]

The TiB_2-reinforced AMCs can remarkably improve the mechanical properties, in particular the stiffness. The typical Young's modulus and other mechanical properties of particulate-reinforced Al/TiB_2 composites are summarized in Table 3. The increase of the Young's modulus of Al/TiB_2 composites can be up to 40% higher than that of pure aluminum.[106,107] The strength at elevated temperatures and the wear and fatigue resistance can also have a significant increase.[108] Kumar et al.[102] reported an increase of 108% in hardness, 123% in yield strength, 43% in UTS, and 33% in Young's modulus of the Al-7Si cast alloy with 10 wt.% of TiB_2, which provides a Young's modulus greater than 90 GPa. Han et al.[108] studied the tensile properties of the Al-12Si alloy with 4 wt.% TiB_2 particles and found that the improvement of the Young's modulus can be observed in the temperature range of 25–350 °C. Amirkhanlou et al.[102] reported that Al-9Si-1Mg-0.7Cu/9 vol.% TiB_2 can provide a Young's modulus greater than 94 GPa and the yield strength up to 235 MPa by the formation of α-Al (Cu, Mg), Si, and TiB_2 phases in the microstructure. Lu et al.[95] investigated the Al/TiB_2 composite and found that the Young's modulus reaches 107 GPa by adding 15% TiB_2 into the Al matrix. Obviously, the main reason for high stiffness properties is formation of high volume fraction TiB_2 with 565 GPa modulus.

3.2. Al/TiC composites

Titanium carbide (TiC) is a hard refractory ceramic material with FCC crystal structures. The Young's modulus is approximately 400 GPa and the shear modulus is 188 GPa for the TiC,[109,110] which is a good candidate as reinforcement for improving stiffness of aluminum alloys[111,112]. Al/TiC *in-situ* composites can be synthesized by several techniques, including: (a) the reaction of K_2TiF_6 salt and graphite, (b) the direct reaction of Ti and C powders, (c) the addition of Al-Ti-C powder into the Al melt, and (d) the reaction of CH_4 gas with the Al-Ti melt. The reactions can be at a level of 1000 °C for 30 minutes for Al-4.5 Cu alloys.[113,114] The *in-situ* formed TiC particles can be smaller than 1 μm in size or in a range of several micrometers.[115,116] The formation of other phases, such as Al_4C_3 and Al_3Ti phases, is considered to be unfavorable in Al/TiC composites.[116,117]

On top of the enhancement of mechanical properties, the addition of TiC particles into aluminum melt has a dramatic improvement on the Young's modulus, as shown in Figure 13. Samer et al.[118] obtained the Young's modulus of 106 GPa, the yield strength of 450 MPa, and the elongation of 6% in the composites containing 22 vol.% TiC in pure Al. Mohapatra et al.[119] confirmed that the Young's modulus is increased from 70 GPa of pure aluminum to 88.78 GPa after adding 20 vol.% TiC. The mechanical properties of Al-4.5%Cu alloy reinforced with different amounts of TiC are summarized in Table 4, in which the addition of 10 wt.% TiC increases the

PROOF ONLY

Table 3. Mechanical properties of Al/TiB_2 cast composites synthesized by K_2TiF_6 and KBF_4 salt reaction.[104,105]

Materials	Temperature (°C)	Young's modulus (GPa)	0.2% Proof stress (MPa)	UTS (MPa)	Elongation (%)
Al-7Si/5 vol.% TiB_2	25	83.0	126	175	7.00
Al-7Si/10 vol.% TiB_2	25	92.0	152	209	4.60
Al-12Si/4 wt.% TiB_2	25	85.0	240	298	1.50
Al-12Si/4 wt.% TiB_2	200	80.0	189	233	3.00
Al-12Si/4 wt.% TiB_2	350	66.0	84	96	5.80
A356/2.1 vol.% TiB_2	25	72.9	209	235	7.81
A356/4.7 vol.% TiB_2	25	76.3	212	252	7.36
A356/8.4 vol.% TiB_2	25	82.2	217	258	2.73
A356/2.1 vol.% TiB_2	25	78.1	305	375	4.88
A356/4.7 vol.% TiB_2	25	80.2	317	377	1.90
A356/8.4 vol.% TiB_2	25	84.1	347	391	1.32
Al/5 vol.% TiB_2	25	69.0	188	284	3.50
Al/10 vol.% TiB_2	25	84.0	249	326	1.92
Al/5 vol.% TiB_2	25	82.0	96	124	9.20
Al/10 vol.% TiB_2	25	87.0	128	164	6.30
Al/15 vol.% TiB_2	25	91.0	124	153	5.50
Al-Cu/10 vol.% TiB_2	25	77.0	153	230	5.50
Al-Cu/10 vol.% TiB_2	25	83.0	311	361	1.30
Al/15 vol.% TiB_2	25	107.0	274	389	1.99
Al/15 vol.% TiB_2	25	91.0	171	223	4.60
Al-Cu/15 vol.% TiB_2	25	93.0	248	333	2.30

Young's modulus to 99 GPa.[121] In addition, the Young's modulus of the Al/TiC composite is close to the upper limit calculated from the Hashin–Shtrikman model,[122,123] suggesting that the *in-situ* synthesis of TiC particles leads to strong interfacial bonding and the attendant load transfer. Despite the high stiffness of Al/TiC *in-situ* composites, the porosity level and other oxide impurities in the melt are the main concerns because of the high synthesis temperature of 1000–1200 °C. High temperature processing also results in limitations for the industrial applications of *in-situ* Al/TiC composites.

3.3. Al/SiC Composites

SiC reinforcements are usually added into Al melt through *ex-situ* additions incorporating with stirring or mixing.[124,125] Casting routes can be gravity casting and squeeze casting. Alternatively, the alloy is infiltrated into a porous preform formed by SiC reinforcements. The wettability between the SiC reinforcements and the aluminum alloy is a crucial concern in association with the optimum fluidity of the alloy. One of the main problems during the processing and casting of Al/SiC composites is that liquid aluminum attacks SiC reinforcements through chemical reaction, forming Al_4C_3 and Si.[126,127] Particle clustering has greater effects on the flow behavior and mechanical properties of Al/SiC AMCs because the particle clustering microstructure experiences a higher percentage of particle fracture than that with particle random distribution.[127,128] The stirring casting is an effective way to promote the distribution of *ex-situ* particles.[129,130]

Table 5 summarizes the Young's modulus and mechanical properties of *ex-situ* Al/SiC AMCs. The

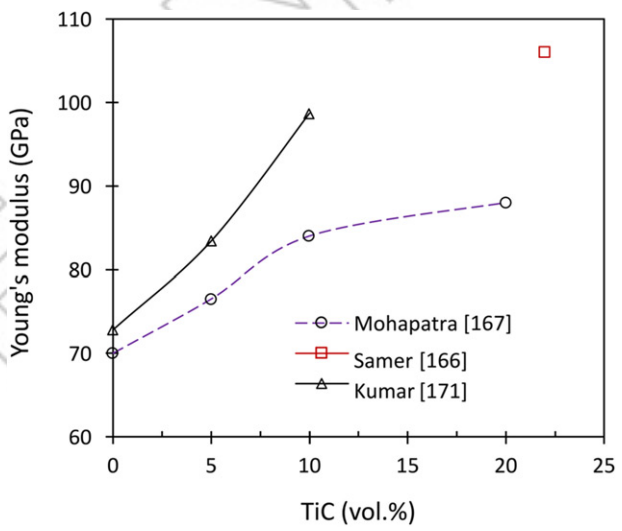

Figure 13. Effect of TiC on the Young's modulus of Al/TiC composites.

Young's modulus of the AMCs with cast aluminum alloys can be enhanced to 114 GPa when the reinforcement is at a level of 20 vol.%. The castability is a significant concern when the SiC addition is beyond this level. For wrought aluminum alloys, the addition of SiC reinforcement can be at a level of 25 vol.% for casting and the subsequent plastic deformation processing. The Young's modulus can be 140 GPa, which is double the Young's modulus of pure aluminum.

3.4. Al/AlN Composites

Aluminum nitride (AlN) has a Young's modulus of 310 GPa and therefore it can fairly increase the modulus of aluminum castings.[132,133] However, because of

PROOF ONLY

Table 4. Mechanical properties of Al matrix and Al-4.5Cu/TiC *in-situ* composites.[120]

Materials	Vickers hardness (HV5)	Young's modulus (GPa)	Yield strength (MPa)	UTS (MPa)
Al-4.5%Cu	55.19	72.8	81.5	118
Al-4.5Cu/5wt.% TiC	61.12	83.4	95.7	134
Al-4.5Cu/7wt.% TiC	69.43	91.8	103.4	156
Al-4.5Cu/10wt.% TiC	75.76	98.7	117.3	179

Table 5. Young's modulus and mechanical properties of *ex-situ* Al/SiC AMCs.[67,131]

Materials	Reinforcement	Casting method	Young's modulus (GPa)	Yield strength (MPa)	UTS (MPa)	Elongation (%)
Al-10Si-3Cu-1Mg-1.25Ni	10 vol.% SiC	Gravity	88	359	372	0.3
Al-10Si-3Cu-1Mg-1.25Ni	20 vol.% SiC	Gravity	101	372	372	0.1
Al-9Si-0.5Mg	10 vol.% SiC	Gravity	86	303	338	1.2
Al-9Si-0.5Mg	20 vol.% SiC	Gravity	99	338	359	0.4
Al-10Si-1Fe-0.6 Mn	10 vol.% SiC	Pressure die cast	91	221	310	0.9
Al-10Si-1Fe-0.6 Mn	20 vol.% SiC	Pressure die cast	108	248	303	0.5
Al-10Si-3.25Cu-1Fe-0.6 Mn	10 vol.% SiC	Pressure die cast	94	241	345	1.2
Al-3.25Cu-1Fe-0.6 Mn	20 vol.% SiC	Pressure die cast	114	303	352	0.4
A356	10 vol.% SiC	Casting	81	283	303	0.6
A356	15 vol.% SiC	Casting	90	324	331	0.3
A356	20 vol.% SiC	Casting	97	331	352	0.4
Al-12Si-Ni-Cu	20 vol.% SiC	Squeeze casting	111	293	384	
Al-7Si-Mg-Fe	15 vol.% SiC	Gravity	98	183	280	1.0
Al-3Mg	20 vol.% SiC	Gravity	105	377	408	1.4
Al-4.4Cu-Si-Mg	15 vol.% SiC	Gravity	107	342	350	1.6
Al-7Si-0.3Mg	10 vol.% SiC	Casting	82	287	308	0.6
Al-7Si-0.3Mg	15 vol.% SiC	Casting	91	329	336	0.3
Al-7Si-0.3Mg	20 vol.% SiC	Casting	98	336	357	0.4
A380	10 vol.% SiC	Casting	95	245	332	1.0
A380	20 vol.% SiC	Casting	114	308	356	0.4
AA6061	20 vol.% SiC	Casting-forming	119	448	551	1.4
AA6061	20 vol.% SiC	Casting-extrusion	108	414	545	2.0
AA6061	20 vol.% SiC	Casting-hot rolling	104	402	550	4.5
AA2014	15 vol.% SiC	Casting-forming	100	466	493	2.0
AA2024	20 vol.% SiC	Casting-forming	110	465	620	2.0
AA2024	25 vol.% SiC	Casting-forming	140	470	800	2.0
AA2024	15 vol.% SiC	Casting-hot rolling	96		530	2.4
AA2024	15 vol.% SiC	Casting-hot rolling	110		330	1.2
AA2618	12 vol.% SiC	Casting-forming	98	460	532	3.0
AA2124	17.8 vol.% SiC	Casting-forming	100	400	610	6.0
AA2124	20 vol.% SiC	Casting-forming	105	405	560	7.0
AA2124	25 vol.% SiC	Casting-forming	116	490	630	3.0
AA7075	15 vol.% SiC	Casting-forming	95	556	601	3.0
AA7075	15 vol.% SiC	Casting-forming	90	598	643	2.0
AA7075	20 vol.% SiC	Casting-forming	105	665	735	2.0
AA8090	13 vol.% SiC	Casting-forming	101	455	520	4.0
AA8090	13 vol.% SiC	Casting-forming	101	499	547	3.0
AA8090	17 vol.% SiC	Casting-forming	105	310	460	5.5
AA8090	17 vol.% SiC	Casting-forming	105	450	540	3.5

the low thermal expansion and good thermal conductivity, Al/AlN is attractive in some specific applications. *In-situ* Al/AlN composites are usually made by a direct reaction between N_2 and/or NH_3 gas with the molten aluminum alloys.[134,135] The nitridation of Al is a thermodynamically exothermic process and is energetically favorable over an extensive temperature range. The formed AlN particles are smaller than 10 μm and show a hexagonal morphology.[136,137] The AlN particles can be less than 2 μm in the Al/AlN composites synthesized by adding NH_3 into the melt in the temperature range from 1,100 to 1,270 °C.[138] In comparison with the purified N_2 bubbling gas, NH_3 can enhance the formation of the AlN phase in aluminum melt.[137] Chedru[139] studied *ex-situ* Al/AlN AMCs with squeeze casting and found that Al/AlN composites can significantly improve the mechanical properties, as shown in Table 6. Balog[139] studied Al/AlN AMCs with cold isostatic pressing (CIP) and extrusion, and the results are shown in Figure 14. The Young's modulus is significantly increased when increasing the content of AlN in the AMCs. However, the studies for castable materials are still very limited

Table 6. Young's modulus and shear modulus of reinforced and non-reinforced materials.[138]

	Young's modulus (GPa)	Shear modulus (GPa)
Al-4Cu-1Mg	72.9	27.1
Al-4Cu-1Mg/45% AlN	146.3	56.5
Al-1Mg-0.5Si	72.5	27.1
Al-1Mg-0.5Si/42% AlN	141.3	54.6
Al-3Mg	71.3	26.6
Al-3Mg/48% AlN	149.5	58.2

PROOF ONLY

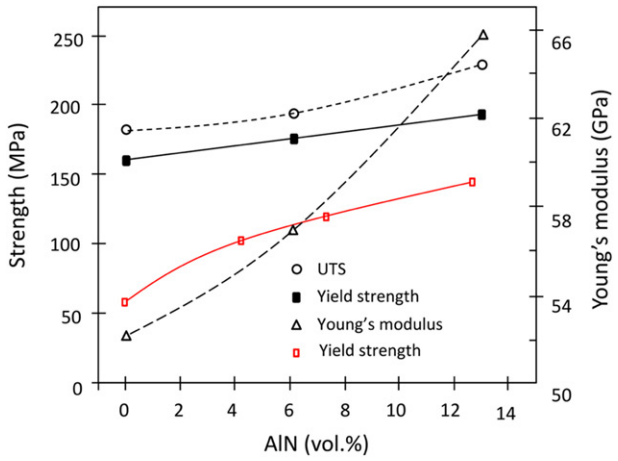

Figure 14. Ultimate tensile strength (UTS), yield strength, and Young's modulus of Al-AlN nanocomposites prepared by CIP with subsequent extrusion.[140]

due to high temperature manufacturing methods for *in-situ* Al/AlN composites.

3.5. Al/ZrB_2-Al_3Zr Composites

Al/ZrB_2-Al_3Zr composites use the hybrid reinforcement phases of ZrB_2 and Al_3Zr. The Young's modulus is 350 GPa for ZrB_2 and 205 GPa for Al_3Zr. Al/ZrB_2-Al_3Zr *in-situ* composites are usually synthesized by the addition of K_2ZrF_6 and KBF_4 salts to Al melt.[141] Zhang et al.[142] synthesized *in-situ* ZrB_2 and Al_3Zr particles in A356 alloy with K_2ZrF_6 and KBF_4 salts. The ZrB_2 and Al_3Zr particles are from 0.3 to 0.5 μm, as shown in Figure 15. Zhao et al.[144] reported that the morphologies of Al_3Zr are sensitive to the temperature of the Al melt. When the temperatures change from 850 to 1000 °C, the morphologies of the Al_3Zr particles can be spherical shape, tetragon shape, rod shape, and fiber shape, but the ZrB_2 particles show no obvious diversity in morphology. The particulate-reinforced Al/ZrB_2-TiB_2 composites can also be formed by the addition of KBF_4, K_2ZrF_6, and K_2TiF_6 salts into Al melt,[145,146] by which the formed TiB_2 and ZrB_2 particles are hexagonal with the average size less than 2 μm.[147]

The Al/ZrB_2-Al_3Zr composites show valuable improvement in stiffness, strength, and wear properties with the increase in ZrB_2 contents.[148,149] As shown in Figure 16, Selvam and Dinaharan[150] verified the stiffness improvement of 7075/ZrB_2 composite, which is further attributed to ZrB_2 that has a covalent interatomic bond and high intrinsic modulus. However, Gautam et al.[151,152] found that the improvement of the Young's modulus in Al/ZrB_2-Al_3Zr hybrid composite is insignificant when the volume

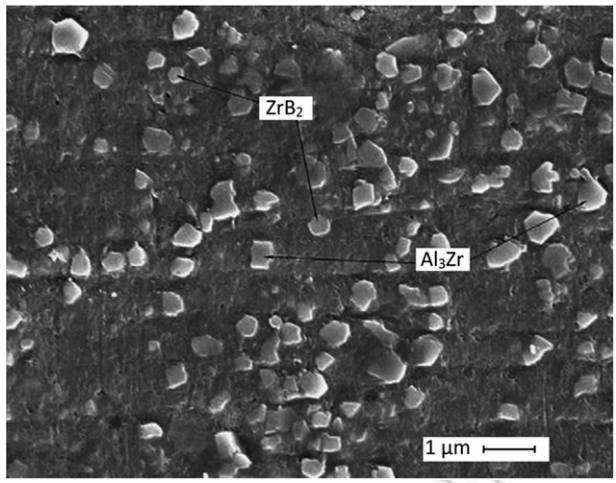

Figure 15. SEM image of the Al/ZrB_2-Al_3Zr hybrid composite.[143]

fraction of ZrB_2 particles increases. The main challenge for fabrication of high modulus *in-situ* composites by casting processes is volume fraction of reinforcement. In fact, it is difficult to form high volume fraction of particles through salt reaction or direct reaction between the gases with the molten aluminum alloys.

3.6. Other Particulate-reinforced AMCs

The other typical reinforcements listed in Table 2 are capable of being synthesized by *in-situ* reactions. However, the compounds with high modulus are more attractive. In addition to that described in the previous section, Al_2O_3, WC, B_4C, and VC are also good candidates for improving the Young's modulus of aluminum composites. For example, the *in-situ* Al/Al_2O_3 composites can be synthesized by: (a) the direct melt oxidation of aluminum alloys at high temperature,[153] (b) directly passing oxygen into the aluminum melt to form Al_2O_3,[154] and (c) the displacement reactions between metal oxides and aluminum to produce Al_2O_3 particulate reinforcement. However, the experimental evidence for the improvement of Young's modulus in those *in-situ* AMCs is not sufficient.

The manufacture and the properties of *ex-situ* AMCs have been comprehensively reviewed by Rohatgi et al.[31] Al/SiC and Al/TiB_2 have also been discussed in the present paper. The other *ex-situ* AMCs processed by casting methods are shown in Table 7. It is possible to combine up to 20 vol.% of $A1_2O_3$ into different aluminum alloys for improving the Young's modulus. The dominant factors in controlling the Young's modulus of *ex-situ* AMCs are the type, shape, volume fraction, and distribution of reinforcement

PROOF ONLY

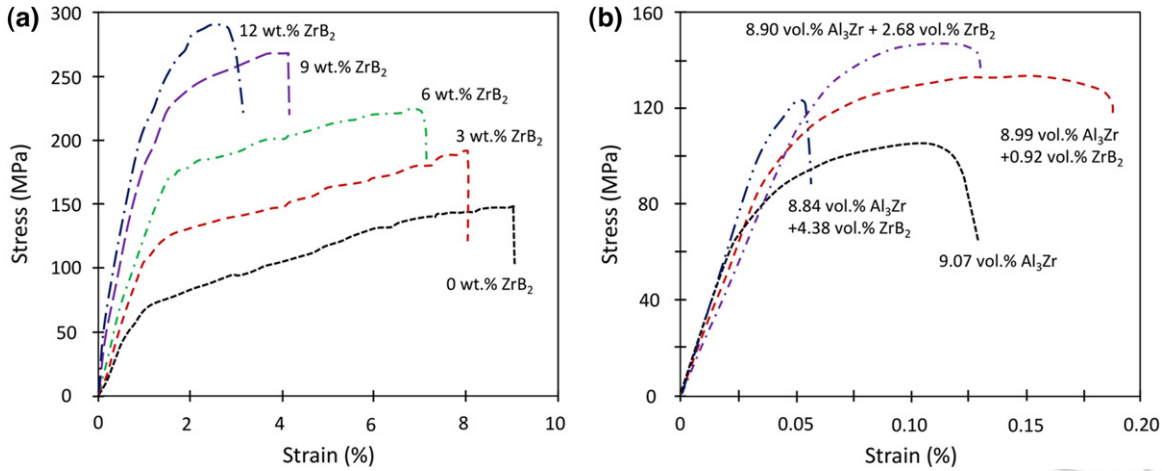

Figure 16. Stress–strain graphs showing: (a) the effect of ZrB_2 content in AA7075/ZrB_2 *in-situ* composites and (b) the effect of ZrB_2 and Al_3Zr content in AA5052/ZrB_2-Al_3Zr *in-situ* composites.[149,150]

Table 7. Young's modulus and mechanical properties of Al-based particulate *ex-situ* composites.[19,66,130]

Materials	Reinforcement	Casting method	Young's modulus (GPa)	YS (MPa)	UTS (MPa)	Elongation (%)
Al-12Si-Ni-Cu	20 vol.% Al_2O_3	Squeeze casting	95	210	297	
Al-4.2Cu-1.4Mg-0.6Ag	25 vol.% Al_2O_3	Stir casting-forming	97	450	460	0.5
Al-4Cu-1Mg-0.5Ag	15 vol.% Al_2O_3	Stir casting-forming	90	414	510	1.3
A201	20 vol.% TiC	Stir casting-forming	105	420		2.0
AA6061	10 vol.% Al_2O_3	Stir casting-forming	81	297	338	7.6
AA6061	15 vol.% Al_2O_3	Stir casting-forming	88	386	359	5.4
AA6061	20 vol.% Al_2O_3	Stir casting-forming	99	359	379	2.1
AA6061	15 vol.% Al_2O_3	Casting-forming	91	342	364	3.2
AA6061	15 vol.% Al_2O_3	Casting-forming	98	405	460	7.0
AA6061	20 vol.% Al_2O_3	Casting-forming	105	420	500	5.0
AA6061	25 vol.% Al_2O_3	Casting-forming	115	430	515	4.0
AA2014	10 vol.% Al_2O_3	Stir casting-forming	84	483	517	3.3
AA2014	15 vol.% Al_2O_3	Stir casting-forming	92	476	503	2.3
AA2014	20 vol.% Al_2O_3	Stir casting-forming	101	483	503	0.9

phases. The porosity and other microstructural characteristics are also critical for property improvement.[155,156] The presence of matrix–particle decohesion, particle cracking, and void growth can decrease the load transfer capability of the interface and, consequently, decrease the Young's modulus of the AMCs. The subsequent mechanical processes are an effective approach to enhance the quality of the interface between matrix and reinforcement in *ex-situ* cast composites as well as the distribution of high modulus particles, as shown in Table 7. Secondary plastic deformation is not capable of altering the Young's modulus of AMCs;[14] however, these processes can improve the toughness of the composites.

The main concern on the Young's modulus of *ex-situ* AMCs is their tendency to have relatively low ductility and fracture toughness, as shown in Table 7. The damage mechanism of *ex-situ* AMCs is mainly the reinforcement fracture and decohesion at the matrix/reinforcement interface. To achieve acceptable ductility and toughness, the composition, heat treatment process, size and shape distribution of the reinforcement should be precisely controlled. Also, secondary mechanical deformation will result in an improvement of ductility. In the presence of strong interfacial bonding, effective load transfer from the matrix to the reinforcement is enhanced, leading to good ductility and damage resistance.

3.7. AMCs with Continuous Reinforcement

Al alloys reinforced with continuous ceramic reinforcement, such as SiC and Al_2O_3, can be considered as alternative materials to achieve outstanding specific strength and modulus. The Al/SiC_p and Al/Al_2O_3 composites can be produced by the molten aluminum infiltration techniques, such as pressure-assisted, vacuum-driven, and pressureless or capillarity-driven processes. Aghajanian et al.[67,157] reported the pressureless infiltration technique, by which the aluminum alloys infiltrated the reinforcement preforms spontaneously in a nitrogen atmosphere. This method is believed to be a cost-effective, nearly net shape technique with the combined processing of

PROOF ONLY

materials and shaping of the components simultaneously. The basic problem encountered in the fabrication of these composites is the rejection of the ceramic phase by the liquid metal due to their lack of wettability.[158] To improve the wetting of ceramics by liquid metals, a possible approach is to apply a metal coating on the ceramic particles, which essentially increases the overall surface energy of the solid, thereby promoting wetting by the liquid metal. Although the continuous ceramic reinforcement/fibers can provide 210 GPa Young's modulus,[159] they usually suffer from very low ductility – less than 0.2 – restricting their applications. Moreover, it is difficult to make shaped castings.

4. Summary and future outlook

The Young's modulus of aluminum-based materials is one of the most important mechanical properties in controlling structural performance. The improvement of the Young's modulus of castable aluminum-based materials is essential for increasing their competiveness in light weighting structural applications. The capability of making complex shaped castings of these materials is critical in considering the massive production and the application in industry. The castability depends on the introduction methods, processing methods, volume fraction, size, and distribution of the high modulus phases. The influence of alloying elements on the Young's modulus depends on the state. If the alloying elements are in a solid solution phase, the magnitude of the Young's modulus is determined by the nature of the atomic interactions. If the alloying elements form second phases, the magnitude of the Young's modulus is determined by the volume fraction and the intrinsic modulus of the second phase. Overall, the increase of Young's modulus in conventional cast aluminum alloys is usually less than 15% through adding alloying elements for manufacturing complex shaped castings. Therefore addition of ceramic particles and reinforcement is necessary for significant improvement of the stiffness of Al alloys.

The improvement of the Young's modulus through introducing high modulus reinforcement phases as AMCs is an effective approach because of their high Young's modulus. The most capable reinforcement phases are TiB_2 (E = 560 GPa) and SiC (E = 480 GPa) for making shaped castings. Reinforcement phases can be added by *ex-situ* or *in-situ* methods, in which the *in-situ* method with particulate reinforcement is preferred for making castings with relatively complex shape and cavity. The main factors governing the Young's modulus of AMCs are the volume fraction, aspect ratio, and the interface. The bonding between the matrix and the reinforcement is the most important factor in determining mechanical properties. Strong interfacial bonding provides effective load transfer from the matrix to the reinforcement for improved Young's modulus and other mechanical properties. The main concern on the performance of AMCs is their tendency to have relatively low ductility and fracture toughness when the materials provide high modulus. When using particulate-reinforced AMCs, the castability should be considered due to challenges in casting components with complex shape and cavity. The balance of castability/processibility and the improvement in Young's modulus is the key for further development.

Bimetallic materials, made by metal wires with cast aluminum alloys, are effective for modulus improvement. In fact, bimetallic materials can be considered a special type of composite material. The preforms made by continuous metallic wires as skeletons or frames are a key step. The pretreatment of the surfaces is needed before casting. The overcasting can be any of the conventional casting methods. Knowledge in this area has not been well established for the variety of preform structures, pretreatments, and casting conditions; so continued study is necessary.

Stiff aluminum alloys are potentially one of the most promising materials for the significant reduction of structural weight with satisfied mechanical properties, including the Young's modulus. There are some knowledge gaps and challenges for the further development of high modulus cast aluminum alloys, which include:

a. The Young's modulus of aluminum alloys with multiple components is not fully understood. The development of complex Al-based alloys with the addition of desirable alloying elements is needed to ensure both high modulus and ductility properties.
b. Up to now, the main purpose for the addition of high modulus phase/reinforcement into the Al alloys has been to improve the wear resistance and high temperature performance. It is very important to carefully and specifically select the type as well as the volume fraction of reinforcement for modulus improvement.
c. Careful selection and combination of desirable alloying elements and *in-situ* formed reinforcement would possibly be the preferred option for developing the material with dominant stiffness properties, toughness, and good castability.

PROOF ONLY

d. In bimetallic materials, reactivity between the reinforcement and the aluminum matrix must be carefully controlled to avoid the formation of brittle interface, which tends to lower the toughness of the interface. Bimetallic materials can be considered for local stiffness improvement of the aluminum components.

Disclosure statement

No potential conflict of interest was reported by the authors.

Funding

Financial support from Jaguar Land Rover (JLR) [grant number R33232] is gratefully acknowledged.

References

1. W. S. Miller, L. Zhuang, J. Bottema, A. Wittebrood, P. De Smet, A. Haszler, and A. Vieregge, Recent development in aluminium alloys for the automotive industry, *Mater. Sci. Eng. A*. **280**(1), 7–49 (2000).
2. T. Dursun and C. Soutis, Recent developments in advanced aircraft aluminium alloys, *Mater. Des*. **56**, 862–871 (2014).
3. D. J. Lloyd, Particle reinforced aluminium and magnesium matrix composites, *Int. Mater. Rev*. **39**(1), 1–23 (1994).
4. J. G. Kaufman and E. L. Rooy, Aluminium alloy castings: properties, processes, and applications, *ASM International*, 2004.
5. F. Bonnet, V. Daeschler, and G. Petitgand, High modulus steels: new requirement of automotive market. How to take up challenge?, *Can. Metall. Q*. **53**, 243–252 (2014).
6. V. S. Zolotorevsky, N. A. Belov, and M. V. Glazoff, *Casting Aluminium Alloys*, Elsevier, Oxford (2007).
7. P. K. Rohatgi, Metal matrix composites, *Def. Sci. J*. **43**(4), 323–349 (2013).
8. A. Mortensen and J. Llorca, Metal matrix composites, *Annu. Rev. Mater. Res*. **40**, 243–270 (2010).
9. S. R. Bakshi, D. Lahiri, and A. Agarwal, Carbon nanotube reinforced metal matrix composites-a review, *Int. Mater. Rev*. **55**, 41–64 (2010).
10. K. L. Kendig and D. B. Miracle, Strengthening mechanisms of an Al-Mg-Sc-Zr alloy, *Acta Mater*. **50**(16), 4165–4175 (2002).
11. K. Masuda-Jindo and K. Terakura, Electronic theory for solid-solution hardening and softening of dilute Al based alloys: elastic-moduli enhancement of Al-Li alloys, *Phys. Rev. B*. **39**(11), 7509 (1989).
12. W. H. Wang, The elastic properties, elastic models and elastic perspectives of metallic glasses, *Prog. Mater. Sci*. **57**, 487–656 (2012).
13. M. Lucena, J. A. Benito, A. Roca, and J. Jorba, Changes of elastomechanic constants of pure aluminum cold deformed by tension test, *Rev. Metal. Madrid*. **34**, 310–313 (1998).
14. A. Villuendas, J. Jorba, and A. Roca, The role of precipitates in the behavior of Young's modulus in aluminium alloys, *Metall. Mater. Trans. A*. **45**(9), 3857–3865 (2014).
15. I. Polmear, D. St John, J. F. Nie, and M. Qian, *Light Alloys: Metallurgy of the Light Metals*. Butterworth-Heinemann (2017).
16. D. Hull and T. Clyne, *An Introduction to Composite Materials*, Cambridge University Press (1996).
17. A. Nieto, A. Bisht, D. Lahiri, and A. Agarwal, Graphene reinforced metal and ceramic matrix composites: a review, *Int. Mater. Rev*. **62**, 241–302 (2017).
18. S. C. Tjong and Z. Y. Ma, Microstructural and mechanical characteristics of *in situ* metal matrix composites, *Mater. Sci. Eng. R*. **29**, 49–113 (2000).
19. I. Ibrahim, F. Mohamed, and E. Lavernia, Particulate reinforced metal matrix composites-a review, *J. Mater. Sci*. **26**, 1137–1156 (1991).
20. R. Jamaati, S. Amirkhanlou, M. R. Toroghinejad, and B. Niroumand, CAR process: a technique for significant enhancement of as-cast MMC properties, *Mater. Charac*. **62**, 1228–1234 (2011).
21. S. Amirkhanlou, R. Jamaati, M. R. Toroghinejad, and B. Niroumand, Manufacturing of high-performance Al356/SiC_p composite by CAR process, *Mater. Manuf. Process*. **26**, 902–907 (2011).
22. F. Lasagni and H. P. Degischer, Enhanced Young's modulus of Al-Si alloys and reinforced matrices by co-continuous structures, *J. Compos. Mater*. **44**, 739–755 (2010).
23. T. Clyne and J. Mason, The squeeze infiltration process for fabrication of metal-matrix composites, *Metall. Trans. A*. **18**(8), 1519–1530 (1987).
24. M. Acilar and F. Gul, Effect of the applied load, sliding distance and oxidation on the dry sliding wear behaviour of Al–10Si/SiCp composites produced by vacuum infiltration technique. *Mater. Des*. **25**(3), 209–217 (2004).
25. Y. Zhang, S. Ji, G. Scamans, and Z. Fan, Interfacial characterisation of overcasting a cast Al-Si-Mg (A356) alloy on a wrought Al-Mg-Si (AA6060) alloy, *J. Mater. Process. Technol*. **243**, 197–204 (2017).
26. X. L. Xie, Y. W. Mai, and X. P. Zhou. Dispersion and alignment of carbon nanotubes in polymer matrix: a review, *Mater. Sci. Eng. R*. **49**, 89–112 (2005).
27. H. Porwal, S. Grasso, and M. J. Reece, Review of graphene-ceramic matrix composites, *Adv. Appl. Ceram*. **112**(8), 443–454 (2013).
28. X. Zhang, W. Chen, H. Luo, and T. Zhou, Formation of periodic layered structure between novel Fe-Cr-B cast steel and molten aluminium, *Scripta Mate*. **130**, 288–291 (2017).
29. S. V. Nair, J. K. Tien, and R. C. Bates. Sic-reinforced aluminium metal matrix composites, *Inter. Met. Rev*. **30**(1), 275–290 (1985).
30. T. Christman and S. Suresh, Microstructural development in an aluminium alloy-SiC whisker composite, *Acta Metall*. **36**(7), 1691–1704 (1988).

PROOF ONLY

31. P. K. Rohatgi, R. Asthana, and S. Das, Solidification, structures, and properties of cast metal-ceramic particle composites, *Inter. Met. Rev.* **31**(1), 115–139 (1986).
32. F. Boland, C. Colin, C. Salmon, and F. Delannay, Tensile flow properties of Al-based matrix composites reinforced with a random planar network of continuous metallic fibres, *Acta Mater.* **46**(18), 6311–6323 (1998).
33. L. Ryelandt, C. Salmon, and F. Delannay, Neutron diffraction analysis of the evolution of phase stresses during plastic straining of aluminium matrix composites reinforced with a continuous, random planar network of fibres, *Mater. Sci. Forum.* **347–349**, 486–491 (2000).
34. Q. Tan, X. Tong, H. Lu, D. Zhang, and J. Hong, Mechanical behaviours of quasi-ordered entangled aluminium alloy wire material, *Mater. Sci. Eng. A.* **527**(1-2), 38–44 (2009).
35. C. Salmon, F. Boland, C. Colin, and F. Delannay, Mechanical properties of aluminium/Inconel 601 composite wires formed by swaging, *J. Mater. Sci.* **33**(23), 5509–5516 (1998).
36. Q. Tan and G. He, 3D entangled wire reinforced metallic composites, *Mater. Sci. Eng. A.* **546**, 233–238 (2012).
37. V. Ganesh, C. Lee, and M. Gupta, Enhancing the tensile modulus and strength of an aluminium alloy using interconnected reinforcement methodology, *Mater. Sci. Eng. A.* **333**(1), 193–198 (2002).
38. C. Salmon, D. Tiberghien, R. Molins, C. Colin, and F. Delannay, Influence of the oxidation conditions of the fibres on the mechanical properties of Al matrix composites reinforced with Ni-based fibres, *Mater. Sci. Forum.* **369–372**, 435–442 (2001).
39. C. Salmon, C. Colin, R. Molins, and F. Delannay, Strengthening of Al/Ni-based composites by *in situ* growth of intermetallic particles, *Mater. Sci. Eng. A.* **334**(1), 193–200 (2002).
40. M. Gupta, M. O. Lai, and C. Y. H. Lim, Development of a novel hybrid aluminium-based composite with enhanced properties, *J. Mater. Process Technol.* **176**(1–3), 191–199 (2006).
41. F. Boland, C. Colin, and F. Delannay, Control of interfacial reactions during liquid phase processing of aluminium matrix composites reinforced with INCONEL 601 fibers, *Metall. Mater. Trans. A.* **29**(6), 1727–1739 (1998).
42. K. Guler, A. Kisasoz, and A. Karaaslan, Investigation of Al/Steel bimetal composite fabrication by vacuum assisted solid mould investment casting, *Acta Phys Polonica A.* **126**(6), 1327–1330 (2014).
43. J. Viala, M. Peronnet, F. Barbeau, F. Bosselet, and J. Bouix, Interface chemistry in aluminium alloy castings reinforced with iron base inserts, *Compos. Part A.* **33**, 1417–1420 (2002).
44. V. Ganesh and M. Gupta, Effect of the extent of reinforcement interconnectivity on the properties of an aluminium alloy, *Scripta Mater.* **44**(2), 305–310 (2001).
45. S. Manasijevic, R. Radiša, Z. Z. Brodarac, N. Dolić, and M. Djurdjevic, Al-Fin bond in aluminium piston alloy & austenitic cast iron insert, *Int. J. Met.* **9**, 27–32 (2015).
46. F. Haddadi, Microstructure reaction control of dissimilar automotive aluminium to galvanized steel sheets ultrasonic spot welding, *Mater. Sci. Eng. A.* **678**, 72–84 (2016).
47. O. Dezellus, B. Digonnet, M. Sacerdote-Peronnet, F. Bosselet, D. Rouby, and J. C. Viala, Mechanical testing of steel/aluminium-silicon interfaces by pushout, *Int. J. Adhes.* **27**, 417–421 (2007).
48. A. Bouayad, C. Gerometta, A. Belkebir, and A. Ambari, Kinetic interactions between solid iron and molten aluminium, *Mater. Sci. Eng. A.* **363**, 53–61 (2003).
49. S. Kobayashi and T. Yakou, Control of intermetallic compound layers at interface between steel and aluminium by diffusion-treatment, *Mater. Sci. Eng. A.* **338**, 44–53 (2002).
50. K. Zhang, X. Bian, Y. Li, Y. Liu, and C. Yang, New evidence for the formation and growth mechanism of the intermetallic phase formed at the Al/Fe interface, *J. Mater. Res.* **95**, 3279–3287 (2013).
51. M. R. Arghavani, M. Movahedi, and A. H. Kokabi, Role of zinc layer in resistance spot welding of aluminium to steel, *Mater. Des.* **102**, 106–114 (2016).
52. Y. Liu, X. Bian, K. Zhang, C. Yang, L. Feng, H. S. Kim, and J. Guo, Interfacial microstructures and properties of aluminium alloys/galvanized low-carbon steel under high-pressure torsion, *Mater. Des.* **64**, 287–293 (2014).
53. T. Liu, Q. Wang, Y. Sui, ~~et al.,~~ An investigation into aluminium–aluminium bimetal fabrication by squeeze casting, *Mater. Des.* **68**, 8–17 (2015).
54. M. Schwankl, J. Wedler, and C. Körner, Wrought Al-Cast Al compound casting based on zincate treatment for aluminium wrought alloy inserts, *J. Mater. Process. Technol.* **238**, 160–168 (2016).
55. S. L. Pramod, S. R. Bakshi, and B. S. Murty, Aluminum-based cast *in situ* composites: a review, *J. Mater. Eng. Perform.* **24**, 2185–2207 (2015).
56. S. Amirkhanlou and B. Niroumand, Fabrication and characterization of Al356/SiC_p semisolid composites by injecting SiC_p containing composite powders, *J. Mater. Process. Technol.* **212**, 841–847 (2012).
57. S. S. Sidhu, S. Kumar, and A. Batish. Metal matrix composites for thermal management: a review, *Crit. Rev. Solid State Mater. Sci.* **4**, 132–157 (2016).
58. B. V. Ramnath, C. Elanchezhian, R. M. Annamalai, S. Aravind, T. S. A. Atreya, V. Vignesh, and C. Subramanian, Aluminium metal matrix composites – a review. *Rev Adv Mater Sci.* 2014;**38**:55–60.
59. K. Tian, Y. Zhao, L. Jiao, S. Zhang, Z. Zhang, and X. Wu, Effects of *in situ* generated ZrB_2 nano-particles on microstructure and tensile properties of 2024 Al matrix composites, *J. Alloys Comp.* **594**, 1–6 (2014).
60. R. Jamaati, S. Amirkhanlou, M. R. Toroghinejad, and B. Niroumand, Comparison of the microstructure and mechanical properties of as-cast A356/SiC MMC processed by ARB and CAR methods, *J. Mater. Eng. Perform.* **21**(7), 1249–1253 (2012).
61. K. U. Kainer, *Basics of Metal Matrix Composites in Book: Metal Matrix Composites: Custom-made*

PROOF ONLY

Materials for Automotive and Aerospace Engineering, 1–54 (2006).
62. K. K. Chawla, *Metal Matrix Composites*, Wiley Online Library (2006).
63. J. Zhang and Z. Fan, Microstructure and mechanical properties of *in situ* Al-Mg_2Si composites. *Mater. Sci. Technol.* **16**(7–8), 913–918 (2000).
64. K. U. Kainer, *Metal Matrix Composites: Custom-made Materials for Automotive and Aerospace Engineering*, John Wiley & Sons (2006).
65. J. Mathew, A. Mandal, and S. D. Kumar, Effect of semi-solid forging on microstructure and mechanical properties of *in-situ* cast Al-Cu-TiB_2 composites, *J. Alloys Comp.* **712**, 460–467 (2017).
66. Z. Fan, Y. Wang, Y. Zhang, T. Qin, X. R. Zhou, G. E. Thompson, T. Pennycook, and T. Hashimoto, Grain refining mechanism in the Al/Al-Ti-B system, *Acta Mater.* **84**, 292–304 (2015).
67. M. K. Aghajanian, M. A. Rocazella, J. T. Burke, and S. D. Keck, The fabrication of metal matrix composites by a pressureless infiltration technique. *J. Mater. Sci.* **26**(2), 447–454 (1991).
68. S. V. Prasad, and R. Asthana, Aluminium metal-matrix composites for automotive applications: tribological considerations, *Tribol. Lett.* **17**(3), 445–453 (2004).
69. S. Amirkhanlou and B. Niroumand, Development of Al356/SiC_p cast composites by injection of SiC_p containing composite powders, *Mater. Des.* **32**(4), 1895–1902 (2011).
70. S. Amirkhanlou and B. Niroumand, Effects of reinforcement distribution on low and high temperature tensile properties of Al356/SiC_p cast composites produced by a novel reinforcement dispersion technique. *Materi. Sci. Eng. A.* **528**(24), 7186–7195 (2011).
71. L. A. Jacobson and J. McKittrick, Rapid solidification processing, *Mater. Sci. Eng. R.* **11**(8), 355–408 (1994).
72. M. Asta, C. Beckermann, and A. Karma, Solidification microstructures and solid-state parallels: recent developments, future directions. *Acta Mater.* **57**(4), 941–971 (2009).
73. K. M. Sree Manu, S. Arun Kumar, T. P. D. Rajan, M. Riyas Mohammed, and B. C. Pai, Effect of alumina nanoparticle on strengthening of Al-Si alloy through dendrite refinement, interfacial bonding and dislocation bowing, *J. Alloys Comp.* **712**, 394–405 (2017).
74. M. L. Ted Guo and C. Y. Tsao, Tribological behaviour of aluminium/SiC/nickel-coated graphite hybrid composites. *Mater. Sci. Eng. A.* **333**, 134–145 (2002).
75. P. K. Rohatgi, K. Pasciak, C. S. Narendranath, et al. Evolution of microstructure and local thermal conditions during directional solidification of A356-SiC particle composites. *J. Mater. Sci.* **29**(20), 5357–5366 (1994).
76. D. Zhao, F. R. Tuler, and D. J. Lloyd, Fracture at elevated temperatures in a particle reinforced composite. *Acta Metall. Mater.* **42**(7), 2525–2533 (1994).
77. Z. Asghar, G. Requena, and E. Boller, Three-dimensional rigid multiphase networks providing high-temperature strength to cast AlSi10Cu5Ni1-2 piston alloys, *Acta Mater.* **59**(16), 6420–6432 (2011).
78. H. Springer, R. Aparicio Fernandez, M. J. Duarte, et al. Microstructure refinement for high modulus *in-situ* metal matrix composite steels via controlled solidification of the system Fe-TiB2, *Acta Mater.* **96**, 47–56 (2015).
79. H. Zhang, H. Springer, R. Aparicio-Fernandez, et al. Improving the mechanical properties of Fe-TiB_2 high modulus steels through controlled solidification processes, *Acta Mater.* **118**, 187–195 (2016).
80. Q. Gao, et al. Improvement of particles distribution of *in-situ* 5 vol% TiB_2 particulates reinforced Al-4.5 Cu alloy matrix composites with ultrasonic vibration treatment, *J. Alloys Comp.* **692**, 1–9 (2017).
81. Q. Gao, et al. Preparation of *in-situ* 5vol% TiB_2 particulate reinforced Al-4.5 Cu alloy matrix composites assisted by improved mechanical stirring process, *Mater. Des.* **94**, 79–86 (2016).
82. G. R. Liu. A step-by-step method of rule-of-mixture of fiber-and particle-reinforced composite materials, *Compos. Struct.* **40**, 313–322 (1997).
83. J. C. Halpin and J. L. Kardos. The Halpin-Tsai equations: a review. *Polymer Eng. Sci.* **16**, 344–352 (1976).
84. Z. Hashin and S. Shtrjkman, A variational approach to the theory of the elastic behaviour of multiphase materials. *J. Mech. Phys. Solids.* **11**, 127–140 (1963).
85. L. Tuchinskii, Elastic constants of pseudoalloys with a skeletal structure, *Powder Metall. Met. Ceram.* **22**, 588–595 (1983).
91. H. Peng, A review of consolidation effects on tensile properties of an elemental Al matrix composite. *Mater. Sci. Eng. A.* **396**, 1–2 (2005).
87. H. B. Michael Rajan, S. Ramabalan, I. Dinaharan, and S. J. Vijay, Synthesis and characterization of *in situ* formed titanium diboride particulate reinforced AA7075 aluminum alloy cast composites, *Mater. Des.* **44**, 438–445 (2013).
88. Z. Liu, et al. Effect of ultrasonic vibration on microstructural evolution of the reinforcements and degassing of *in situ* TiB_{2p}/Al-12Si-4Cu composites, *J. Mater. Process. Technol.* **212**(2), 365–371 (2012).
89. J. Geng, et al. The solution treatment of *in-situ* submicron TiB_2/2024 Al composite, *Mater. Des.* **98**, 186–193 (2016).
90. T. Hong, Y. Shen, J. Geng, et al. Effect of cryogenic pre-treatment on aging behavior of *in-situ* TiB_2/Al–Cu–Mg composites, *Mater. Charac.* **119**, 40–46 (2016).
91. K. Tee, L. Lu, and M. Lai, *In situ* stir cast Al-TiB_2 composite: processing and mechanical properties, *Mater. Sci. Technol.* **17**(2), 201–206 (2001).
92. K. L. Tee, L. Lu, and M. Lai, *In situ* processing of Al-TiB_2 composite by the stir-casting technique, *J. Mater. Process. Technol.* **89**, 513–519 (1999).
93. K. Tee, L. Lu, and M. Lai, Synthesis of *in situ* Al-TiB_2 composites using stir cast route, *Compos. Struct.* **47**(1), 589–593 (1999).
94. A. Changizi, A. Kalkanli, and N. Sevinc, Production of *in situ* aluminium–titanium diboride master alloy

PROOF ONLY

formed by slag–metal reaction, *J. Alloys Comp.* **509**(2), 237–240 (2011).
95. L. Lü, et al. *In situ* TiB_2 reinforced Al alloy composites, *Scripta Mater.* **45**(9), 1017–1023 (2001).
96. J. Mathew, et al. X-ray tomography studies on porosity and particle size distribution in cast *in-situ* Al-Cu-TiB_2 semi-solid forged composites, *Mater. Charact.* **118**, 57–64 (2016).
97. A. Mandal, M. Chakraborty, and B. Murty, Ageing behaviour of A356 alloy reinforced with *in-situ* formed TiB_2 particles, *Mater. Sci. Eng. A.* **489**(1), 220–226 (2008).
98. C. Feng and L. Froyen, Microstructures of *in situ* Al/TiB_2 MMCs prepared by a casting route, *J. Mater. Sci.* **35**(4), 837–850 (2000).
99. X. H. Chen and H. Yan, Solid–liquid interface dynamics during solidification of Al 7075-Al_2O_{3np} based metal matrix composites, *Mater. Des.* **94**, 148–158 (2016).
100. Z. Chen, et al. Development of TiB_2 reinforced aluminium foundry alloy based *in situ* composites – Part I: an improved halide salt route to fabricate Al-5wt% TiB_2 master composite, *Mater. Sci. Eng. A.* **605**, 301–309 (2014).
101. A. Mandal, B. Murty, and M. Chakraborty, Sliding wear behaviour of T6 treated A356-TiB_2 *in-situ* composites, *Wear.* **266**(7), 865–872 (2009).
103. S. Amirkhanlou, S. Ji, Y. Zhang, et al. High modulus Al-Si-Mg-Cu/Mg_2Si-TiB_2 hybrid nanocomposite: microstructural characteristics and micromechanics-based analysis, *J. Alloy Compd.* **694**, 313–324 (2017).
106. A. Westwood, Materials for advanced studies and devices. *Metall. Trans. A.* **19**(4), 749–758 (1988).
107. G. Li, M. Zheng, and G. Chen, Mechanism and kinetic model of *in-situ* TiB_2/7055Al nanocomposites synthesized under high intensity ultrasonic field, *J. Wuhan Uni. Technol. Mater. Sci. Ed.* **26**(5), 920–925 (2011).
102. S. Kumar, et al. Tensile and wear behaviour of *in situ* Al-7Si/TiB_2 particulate composites, *Wear.* **265**(1), 134–142 (2008).
108. G. Han, et al. High-temperature mechanical properties and fracture mechanisms of Al-Si piston alloy reinforced with *in situ* TiB_2 particles, *Mater. Sci. Eng. A.* **633**, 161–168 (2015).
104. S. Kumar, V. S. Sarma, and B. Murty, Effect of temperature on the wear behaviour of Al-7Si-TiB_2 *in-situ* composites, *Metall. Mater. Trans. A.* **40**(1), 223–231 (2009).
105. M. Wang, et al. Mechanical properties of *in-situ* TiB_2/A356 composites, *Mater. Sci. Eng. A.* **590**, 246–254 (2014).
109. R. Chang and L. J. Graham, Low-temperature elastic properties of ZrC and TiC, *J. Applied Phys.* **37**(10), 3778–3783 (1966).
110. W. Jiang, et al. Synthesis of TiC/Al composites in liquid aluminium, *Mater. Lett.* **32**(2), 63–65 (1997).
111. K. J. Lijay, et al. Microstructure and mechanical properties characterization of AA6061/TiC aluminium matrix composites synthesized by *in situ* reaction of silicon carbide and potassium fluotitanate, *Trans. Nonferrous Met. Soc. China.* **26**(7), 1791–1800 (2016).
112. J. J. Moses, I. Dinaharan, and S. J. Sekhar, Prediction of influence of process parameters on tensile strength of AA6061/TiC aluminum matrix composites produced using stir casting, *Trans. Nonferrous Met. Soc. China.* **26**, 1498–1511 (2016).
113. Y. Liang, J. Zhou, and S. Dong, Microstructure and tensile properties of *in situ* TiC_p/Al-4.5 wt.% Cu composites obtained by direct reaction synthesis, *Mater. Sci. Eng. A.* **527**(29), 7955–7960 (2010).
114. Z. Liu, et al. Synthesis of submicrometer-sized TiC particles in aluminium melt at low melting temperature, *J. Mater. Res.* **29**(7), 896–901 (2014).
115. P. Li, E. Kandalova, and V. Nikitin, *In situ* synthesis of Al-TiC in aluminium melt, *Mater. Lett.* **59**(19), 2545–2548 (2005).
117. R. Tyagi, Synthesis and tribological characterization of *in situ* cast Al-TiC composites, *Wear.* **259**(1), 569–576 (2005).
116. B. Yang, G. Chen, and J. Zhang, Effect of Ti/C additions on the formation of Al_3Ti of *in situ* TiC/Al composites, *Mater. Des.* **22**(8), 645–650 (2001).
118. N. Samer, et al. Microstructure and mechanical properties of an Al-TiC metal matrix composite obtained by reactive synthesis, *Compos. Part A.* **72**, 50–57 (2015).
119. S. Mohapatra, et al. Fabrication of Al-TiC composites by hot consolidation technique: its microstructure and mechanical properties, *J. Mater. Res. Technol.* **5**(2), 117–122 (2016).
121. A. P. Amosov, A. Luts, and A. Ermoshkin, Nanostructured aluminium matrix composites of Al-10% TiC obtained *in situ* by the SHS method in the melt, *Key Eng. Mater.* **684**, 281–286 (2016).
122. Z. Hashin and S. Shtrikman, A variational approach to the elastic behaviour of multiphase materials, *J. Mech. Phys. Solid.* **11**, 127–140 (1962).
123. X. Tong and H. Fang, Al-TiC composites *in situ*-processed by ingot metallurgy and rapid solidification technology: Part II. Mechanical behaviour, *Metall. Mater. Trans. A.* **29**(3), 893–902 (1998).
120. A. Kumar, P. Jha, and M. Mahapatra, Abrasive wear behaviour of *in Situ* TiC reinforced with Al-4.5% Cu matrix, *J. Mater. Eng. Perform.* **23**(3), 743–752 (2014).
124. S. Amirkhanlou and B. Niroumand, Synthesis and characterization of 356-SiCp composites by stir casting and compocasting methods, *Trans. Nonferrous Met. Soc. China.* **20**, s788–s793 (2010).
125. S. Amirkhanlou, R. Jamaati, B. Niroumand, and M. R. Toroghinejad, Using ARB process as a solution for dilemma of Si and SiC_p distribution in cast Al–Si/SiC_p composites, *J. Mater. Process. Technol.* **211**, 1159–1165 (2011).
126. J. C. Lee, J. Y. Byun, S. B. Park, et al. Prediction of Si contents to suppress the formation of Al_4C_3 in the SiC_p/Al composite, *Acta Mater.* **46**(5), 1771–1780 (1998).
127. S. Amirkhanlou and B. Niroumand, Microstructure and mechanical properties of Al356/SiC_p cast composites fabricated by a novel technique, *J. Mater. Eng. Perform.* **22**(1), 85–93 (2012).
128. Z. Peng and L. Fuguo, Effects of particle clustering on the flow behaviour of SiC particle reinforced Al

PROOF ONLY

metal matrix composites, *Rare Met. Mater. Eng.* **39**(9), 1525–1531 (2010).
129. S. Balasivanandha Prabhu, L. Karunamoorthy, S. Kathiresan, et al. Influence of stirring speed and stirring time on distribution of particles in cast metal matrix composite, *Mater. Process. Technol.* **171**, 268–273 (2006).
130. S. Tzamtzis, N. S. Barekar, N. Hari Babu, et al. Processing of advanced Al/SiC particulate metal matrix composites under intensive shearing-A novel Rheo-process, *Compos. Part A*. **40**, 144–151 (2009).
131. A. H. Properties, *Selection: Nonferrous Alloys and Special-purpose Materials*, vol. **2**, ASM International, Materials, Park, OH (1990).
132. B. A. Kumar and N. Murugan, Metallurgical and mechanical characterization of stir cast AA6061-T6–AlN_p composite, *Mater. Des.* **40**, 52–58 (2012).
133. P. Yu, et al. *In situ* fabrication and mechanical properties of Al-AlN composite by hot extrusion of partially nitrided AA6061 powder, *J. Mater. Res.* **26**(14), 1719–1725 (2011).
134. C. Yang, et al. Microstructure and mechanical properties of AlN particles *in situ* reinforced Mg matrix composites, *Mater. Sci. Eng. A*. **674**, 158–163 (2016).
135. Q. Hou, R. Mutharasan, and M. Koczak, Feasibility of aluminium nitride formation in aluminium alloys, *Mater. Sci. Eng. A*. **195**, 121–129 (1995).
136. Q. Zheng and R. Reddy, Mechanism of *in situ* formation of AlN in Al melt using nitrogen gas, *J. Mater. Sci.* **39**(1), 141–149 (2004).
137. S. S. Kumari, U. Pillai, and B. Pai, Synthesis and characterization of *in situ* Al-AlN composite by nitrogen gas bubbling method, *J. Alloy Compd.* **509**(5), 2503–2509 (2011).
138. Q. Zheng and R. G. Reddy, Kinetics of *in-situ* formation of AlN in Al alloy melts by bubbling ammonia gas, *Metall. Mater. Trans. B.* **34**(6), 793–804 (2003).
139. M. Chedru, J. L. Chermant, and J. Vicens, Thermal properties and Young's modulus of Al-AlN composites, *J. Mater. Sci. Lett.* **20**, 893–895 (2001).
140. M. Balog, P. Krizik, M. Yan, et al. SAP-like ultrafine-grained Al composites dispersion strengthened with nanometric AlN, *Mater. Sci. Eng. A*. **588**, 181–187 (2013).
141. I. Dinaharan, N. Murugan, and S. Parameswaran, Influence of *in situ* formed ZrB_2 particles on microstructure and mechanical properties of AA6061 metal matrix composites, *Mater. Sci. Eng. A*. **528**(18), 5733–5740 (2011).
142. S. L. Zhang, et al. Fabrication and dry sliding wear behaviour of *in situ* Al-K_2ZrF_6-KBF_4 composites reinforced by Al_3Zr and ZrB_2 particles, *J. Alloy Compd.* **450**(1), 185–192 (2008).
144. Y. Zhao, et al. Effects of molten temperature on the morphologies of *in situ* Al_3Zr and ZrB_2 particles and wear properties of $(Al_3Zr + ZrB_2)$/Al composites, *Mater. Sci. Eng. A*. **457**(1), 156–161 (2007).
145. D. Zhao, et al. *In-situ* preparation of Al matrix composites reinforced by TiB_2 particles and sub-micron ZrB_2, *J. Mater. Sci.* **40**(16), 4365–4368 (2005).
146. N. Rengasamy, M. Rajkumar, and S. S. Kumaran, An analysis of mechanical properties and optimization of EDM process parameters of Al 4032 alloy reinforced with ZrB_2 and TiB_2 *in-situ* composites, *J. Alloy Compd.* **662**, 325–338 (2016).
147. A. Mahamani, et al. Synthesis, quantitative elemental analysis, microstructure characteristics and micro hardness analysis of AA2219 aluminium alloy matrix composite reinforced by *in-situ* TiB_2 and sub-micron ZrB_2 particles, *Frontiers Auto Mech. Eng.* **25**, 50–53 (2010).
143. S. Zhang, Y. Zhao, G. Chen, and X. Cheng, Microstructures and dry sliding wear properties of *in situ* $(Al_3Zr + ZrB_2)$/Al composites, *J. Mater. Process. Technol.* **184**, 201–208 (2007).
148. I. Dinaharan and N. Murugan, Dry sliding wear behaviour of AA6061/ZrB_2 *in-situ* composite, *Trans. Nonferrous Met. Soci. China*. **22**(4), 810–818 (2012).
149. G. N. Kumar, et al. Dry sliding wear behaviour of AA 6351-ZrB_2 *in situ* composite at room temperature, *Mater. Des.* **31**(3), 1526–1532 (2010).
150. J. D. R. Selvam and I. Dinaharan, *In situ* formation of ZrB_2 particulates and their influence on microstructure and tensile behaviour of AA7075 aluminium matrix composites, *Eng. Sci. Technol. Inter. J.* **20**(1), 187–196 (2017).
151. G. Gautam, et al. High temperature tensile and tribological behaviour of hybrid $(ZrB_2 + Al_3Zr)$/AA5052 *in situ* composite, *Metall. Mater. Trans. A*. **47**(9), 4709–4720 (2016).
152. G. Gautam and A. Mohan, Effect of ZrB_2 particles on the microstructure and mechanical properties of hybrid $(ZrB_2 + Al_3Zr)$/AA5052 *in situ* composites, *J. Alloy Compd.* **649**, 174–183 (2015).
153. K. Wang, et al. Fabrication of *in situ* AlN-TiN/Al inoculant and its refining efficiency and reinforcing effect on pure aluminium, *J. Alloy Compd.* **547**, 5–10 (2013).
154. Y. Zhang, N. Ma, and H. Wang, Improvement of yield strength of LM24 alloy, *Mater. Des.* **54**, 14–17 (2014).
155. S. Amirkhanlou, M. R. Rezaei, B. Niroumand, and M. R. Toroghinejad, High-strength and highly-uniform composites produced by compocasting and cold rolling processes, *Mater. Des.* **32**, 2085–2090 (2011).
156. P. D. Lee and J. D. Hunt, Hydrogen porosity in directional solidified aluminium-copper alloys: *in situ* observation, *Acta Mater.* **45**(10), 4155–4169 (1997).
157. M. K. Aghajanian, J. Burke, D. R. White, et al. A new infiltration process for the fabrication of metal matrix composites, *SAMPE Quarterly*. **20**, 43–46 (1989).
158. J. Chen, C. Hao, and J. Zhang, Fabrication of 3D-SiC network reinforced aluminium-matrix composites by pressureless infiltration, *Mater. Lett.* **60**, 2489–2492 (2006).
159. G. S. Daehn, B. Starck, and L. Xu, Elastic and plastic behaviour of a co-continuous alumina/aluminium composite, *Acta Mater.* **44**, 249–261 (1996).
160. B. Basu and K. Balani. *Advanced Structural Ceramics*. John Wiley & Sons (2011).

PROOF ONLY